geet Green Energy and Environmental Technology

IntechOpen Journals

REVIEW PAPER

Comprehensive Investigation of Perovskite Materials for Photocatalytic, Photovoltaic, and Optoelectronic Applications: Recent and Advance Challenges and Goals

Shoukat Hussain* and Muhammad Muzammal Shahid

Institute of Physics, Khwaja Fareed University of Engineering and Information Technology, Rahim Yar Khan, Pakistan
*Correspondence: E-mail: 010shoukat@gmail.com

Citation
Shoukat Hussain and Muhammad Muzammal Shahid (2024), Comprehensive Investigation of Perovskite Materials for Photocatalytic, Photovoltaic, and Optoelectronic Applications: Recent and Advance Challenges and Goals. *Green Energy and Environmental Technology* 3(1), 1–51.

DOI
https://doi.org/10.5772/geet.30

Received: 26 December 2023
Accepted: 18 June 2024
Published: 1 August 2024

Abstract

Energy and environment are two of the most important issues of our time on a worldwide scale. Photocatalysis is the most environmentally friendly answer to these issues. Perovskite-based materials have sparked attention due to their low cost and lack of toxicity. Substitutable solar energy and semiconductor photocatalytic technologies are two of the most essential ways to reduce or avert global catastrophes and energy concerns. It is estimated that over one thousand different materials such as $KGaO_3$ and $RbMg_2Ti_3O_{10}$ have been tested for their potential as photocatalysts recently. Among the many endeavors, the production of photocatalysts is seen as a crucial technique for using solar energy for long-term energy and environmental reasons. Many photocatalysts ($RbGaO_3$) have previously been combined. A photoelectrochemical cell is a device that converts light to electricity via a photoelectrochemical reaction. The sun is the major source of our power. Clean hydrogen energy is generated by a photocatalyst, which removes both inorganic and organic contaminants from water. Photocatalysts that operate over the whole solar spectrum have been developed as a result of significant advances in this area. Among the various materials that have been produced so far, single- and double-perovskite-based materials have received a lot of attention.

Keywords: perovskite, photocatalytic, photochemical reaction, hydrogen, challenges

1. *Introduction*

By definition, a perovskite is a material with a crystal structure that is comparable to $CaTiO_3$, $SrTiO_3$, $CaSiO_3$, or $BaTiO_3$. The genesis of perovskite may be traced back to 1839, when a German scientist Gustav Rose found a novel $CaTiO_3$ mineral in the Ural Mountains, which was dubbed "perovskite" in honor of the Russian mineralogist Lev von Perovski [1]. The number of applications based on photocatalysis has expanded dramatically during the past two decades, and a wide spectrum of the material system has been created [2]. Photocatalysis has sparked interest due to the utilization of solar energy to create hydrogen from water [3]. A general compound ABO_3 is included in the general formula of perovskites. The larger cation normally occupies the A-site in this crystalline form, whereas the smaller cation occupies the B-site. Perovskites are a significant family of materials with properties that make them excellent for a wide variety of technological applications [4]. Perovskite photocatalysts have been intensively explored due to their ability to be active in visible light. An overview of current work on visible-range-driven perovskite photocatalysts [5] is necessary to offer a broad viewpoint and possible future methods. Shietal gave an overview of photocatalysts made of perovskite that work in both ultraviolet (UV) and visible light [6]. The key advantages of photocatalysis [7] are as follows: efficiency at room temperature, the use of renewable and clean solar power as the driving energy, and any hazardous waste generation after mineralization to match the industry's "nonexistent" waste system [8]. The standard perovskite formula is ABX_3. The organic cation hits the HOIP A-site; the group IVA metal in divalent oxidation form targets the B-site; the halogen anion attacks the X-site. As previously reported [9], the B–X bonds are largely responsible for the electrical properties of the characterized perovskites. Electronic properties are critical for understanding heterogeneous photocatalysis [10]. We focused on optical, electronic, structural, and compact aspects of this family of promising photocatalytic materials [11]. The initial benefits of the structures are the low cost of fabrication, minimization of local integration, the length of electron–hole long shallow points, charge separation, and right grain boundary owing to the element's considerable tolerance. Second, these devices have a reputation for absorbing light switches while maintaining the proper bandgap [12]. Low-cost management approaches may also be used to create them [13]. The existence of a catalyst surface in the visual environment, as well as light source input, which activates the picture in the system, can affect this behavior. The extent of active site acquisition increased when the catalyst was added whereas both light penetration and the number of filtered particles   decreased [14]. Moreover, a high quantity of the catalyst may cause particles to collide with molecules on the surface, decreasing the reaction rate. The trade-offs between these consequences were carefully evaluated, with an emphasis on pollution. Perovskite photocatalysts have been extensively explored due to their visible light potential. By analyzing current activity in visible-light-driven perovskite photocatalysts, regular investigations of the perovskite photocatalysts functional under visible light and UV [13] present larger future prospects and perspective methods. The current review focuses on the visible-light photocatalysis of perovskite compounds. The ways for increasing or augmenting visible light absorption and, as a result, photocatalytic activity are discussed [15]. Furthermore, we want to clarify essential ideas linked to the structure of the crystal perovskite that play a key role in photocatalytic activities, highlighting areas of possible study in the field. The first portion of the article discusses the thermodynamics and processes of the most prevalent photocatalytic reactions while the second section delves further into material systems [16]. In this review, perovskite is divided into two types: simple perovskite (like ABO_3) and sophisticated perovskite (like ABO_4; thickened, double, etc.) [17]. Furthermore, we want to clarify essential ideas linked to the structure of crystal perovskite that play a key role in photocatalytic processes, highlighting areas of possible study in the field. The article's first portion covers the thermodynamics and mechanics of the most frequent photocatalytic reactions while the second section delves further into material systems. In this review, perovskite is divided into two types: complex perovskite and simple perovskite (type ABO_3). (It has been copied, thickened, and so on.) $CaTiO_3$ is one of the most common perovskite minerals, with a bandgap of 3.6 eV. Light-driven water deterioration has been described [18], and Cu doping in calcium titanate has been intensively explored. Cu doping promotes light absorption and improves hydrogen exposure to UV radiation when using the NiO_x cocatalyst [19]. For the development of effective photocatalysts, the study of doped systems in which dopants form photocatalytic receptors is crucial. The negative effects of doping on structures, such as electron–hole recombination, active electron/hole mass, and reduced gloss, should be carefully explored and documented. This study is useful for understanding more about the photocatalytic activity of doped systems. La and Ag codoping on $CaTiO_3$ was done to minimize the bandgap, resulting in light absorption [16]. According to density functional theory experiments, $CaTiO_3$-restricted titanium dioxide (TiO_2) sites, such as $SrTiO_3$, can absorb light. A few metal titanates, particularly alkaline titanates, show promise as photocatalysts in visible light. Perovskite, bismuth, cobalt, nickel, and antimony are some more photocatalysts with noticeable bandgap values (the site that remains B). Pentavalent bismuth perovskite is a photocatalyst that is active in visible light. Perovskites include $NaBiO_3$ (2.53 eV), $LiBiO_3$ (1.63 eV), $KGaO_3$ (2.74 eV) [20], $KBiO_3$ (2.04 eV), and $AgBiO_3$ (2.04 eV).

Graphitic carbon nitride is a nonoxide semiconductor with a large bandgap that can produce hydrogen by photoelectrochemical (PEC) water splitting (WS). This work evaluates the PEC WS efficiency of a g-C_3N_4 nanoflake film produced through thermal pyrolysis. FESEM and XRD investigations validate the nanoflake's shape and graphitic phase of C_3N_4, which has a median crystallite size of 8.49 nm. A spectrophotometer with a UV–visible wavelength is used to estimate the photoanode film's E_g (2.7 eV). The manufactured g-C_3N_4 film exhibits a photocurrent density of 0.87 lA/cm² under UV irradiation [21]. $BaTiO_3$ NPs are placed in a zeolitic imidazolate framework (ZIF-8) to form $BaTiO_3$ nanocomposites that may degrade methylene blue photocatalytically under sun irradiation. To assist the smooth transfer of charges between $BaTiO_3$, enabling ZIF-8 to develop on the surface of $BaTiO_3$. The concentration of $BaTiO_3$ is changed throughout production to improve photocatalytic activity [22]. The primary purpose of this study is to investigate the rheological properties of hybrid nanolubricants (HNLs) with different compositional ratios in a base oil. The study aims to identify the HNL that provides optimal lubrication at motor startup. Theoretical approaches have confirmed non-Newtonian behavior under various lab conditions. The HNLs with composition ratios of 30:70 and 25:75 show the greatest rise and fall in the viscosity percentage, respectively [23]. The PVDF is the preferred ferroelectric supporting or membrane element. The LSMO is a well-known electrode material for solid oxide fuel cells. Using silver nitrate and a reduction agent, four polymer composites made of PVDF–LSMO–PANI were created with varying amounts of silver doping. The characterization of these four new PVDF-based compounds was done using FTIR, XRD, SEM, and UV–visible DRS. The current presentation focuses on the influence of PANI in the PVDF–LSMO–PANI composite on the photocatalytic degradation of ciprofloxacin [24].

2. *Brief sketch of perovskite material in photocatalysis*

The term "photocatalysis," which has been around for about a century, refers to the change in the rate of a chemical reaction caused by the action of light in the presence of a catalyst that absorbs light and participates in chemical reactions. There are two words in photocatalyst: photon and catalyst [25]. When a photocatalyst interacts with a light source, it alters the rate of the chemical reaction by absorbing light energy. When light is absorbed by the substrate, it serves as the catalyst for chemical reactions. Semiconductors make up all photocatalysts [26]. In photocatalysis, a semiconducting device is exposed to light and an electron–hole pair is formed. This type of reaction is called homogeneous photocatalysis if it occurs when both the semiconductor and the reactant are in the same phase (i.e. a gas, solid, or liquid).

Heterogeneous photocatalysis refers to photocatalytic reactions in which the semiconductor and reactant are in different phases. Among the many applications of photocatalysts are preservation and energy conservation, the elimination of odors, sterilization, and self-cleansing and water purification. Due to their electronic structure, semiconductors serve as photoredox process sensors. Organic matter such as aromatics, pesticides, dyes, halo hydrocarbons, and surfactants can be photocatalyzed by some semiconductors [27], resulting in their complete mineralization. There are three main categories of photocatalysts: zinc oxide, titanium dioxide, and other metal oxides (such as molybdenum oxide and vanadium dioxide). TiO_2, V_2O_5, ZnO, Fe_2O_3, CdO, and CdS have been used as heterogeneous binary metal oxide photocatalysts for the few decades of Al_2O_3. Due to its extensive availability, low toxicity, cheap cost, and other well-known properties, TiO_2 is a commonly used photocatalyst [28, 29]. Electrons in TiO_2 that are excited by UV light are conveyed to the conductor band when the wavelength is between 200 and 400 nm. Thus, an oxidative/reductive reaction cycle is generated as additional electron–hole pairs are produced throughout this process. The UVA radiation is only approximately 5% of the sun's rays at that time, which means that the photon's effectiveness in sunlight is much lower [30]. As a consequence, its use on a large scale is economically constrained. To make the perovskite work, UV light is needed although artificial light sources may also be supplemented with sunshine. There has been a surge in interest in the application of perovskite photocatalysis to remove drugs from water and wastewater due to the efficient destruction of numerous drug classes. Catalyst loading, initial substrate concentration, perovskite photocatalyst type, solution pH, wavelength/light intensity, and water matrix in decay are only a few of the performance factors that are often studied in perovskite photocatalytic investigations. Also addressed in this study are the impacts of traveling speed as well as the temperature and gas depletion rates. Micropollutants and microbiological pathogens are eliminated by oxidative means in water and wastewater treatment. It has low toxicity, high stability, and photocatalytic activity as $KGaO_3$ and $RbMg_2Ti_3O_{10}$ [20, 31] in the UV and potentially visible ranges. Recently, researchers, utilizing a photocatalytic membrane reactor (PMR), have been conducting a wide range of studies to analyze the merging process and catalysis, filter water, and store catalytic particles. An attempt to ensure complete rejection of any possibly harmful nanoparticles would need extremely effective photocatalytic microscopic particles and an appropriate filtering mechanism, such as nanofiltration (NF). In addition, the high-pressure pump required to implement this technology is prohibitively costly [32]. In order to work below the wavelength of 495 nm, photocatalytic devices should have a bandgap of 2.42 eV. For the *n*-type photocatalytic titanium, the bandgap is 3.0 eV [33].

2.1. Photocatalytic CO_2 reduction

When carbon dioxide (CO_2) concentrations increase, it puts the environment at risk as global warming and air pollution rise to unsafe levels. After increasing at an annual pace of more than 2 ppm during the previous decade, carbon dioxide levels reached 400 ppm in 2015 [34]. It is now widely accepted that lowering carbon dioxide concentrations and emissions in the atmosphere is essential for the long-term survival of humanity. Climate change is mostly the result of human activity, industrialization, and the use of fossil fuels. Conserving fossil fuels and converting atmospheric CO_2 into valuable products are two ways to reduce global CO_2 emissions. Carbon dioxide is a stable molecule from a thermodynamic standpoint because of the higher binding separation energy of the CO bond (750 kJ/mol) compared to the CH (336 kJ/mol) and CC (411 kJ/mol) bonds [35]. As a consequence, the CO_2 molecule is exceedingly stable, and breaking this CO bond for subsequent reactions requires a large amount of energy. In contrast, the activation of CO_2 by traditional thermocatalysis consumes a significant amount of energy and results in secondary pollutants owing to the high temperatures required. CO_2 is fixed in nature through the process of photosynthesis, where sunlight causes green plants to produce oxygen and glucose from water and CO_2. As a long-term answer to this problem, carbon dioxide photocatalytic reduction was developed [36]. Hydrocarbon fuels like CH_4, CH_3OH, and, C_2H_5OH may be prepared from CO_2 by capturing a large amount of solar energy [37]. These carbonaceous chemicals' synthesis requires more electrons in terms of kinetics than does CO_2 reduction's main competitor, hydrogen evolution. Furthermore, mass-transfer restrictions for the synthesis of these carbonaceous compounds exist owing to CO_2's restricted water solubility.

Photocatalytic CO_2 reduction, on the other hand, is beneficial to both the environment and the economy [39]. Different products may be produced in this process depending on the probability of the available protons and electrons. Multielectron photocatalysis, however, has been shown to be less dependable than a free electron process, which includes numerous steps but only one final result. The first step in carbon dioxide reduction is the generation of $CO_2^{\bullet-}$ radical anions (1.9 eV vs NHE, at pH 7), which is unachievable for most perovskites because of their less-negative conduction band (CB) potentials. Since CO_2 reduction has a high activation energy (E) and inactive kinetics, the reaction takes longer. But CO_2 adsorption on the active photocatalyst's surface assists the reduction reaction by forming charged CO_2, which decrease the energy (E) barrier to absorb the electrons that are being produced [40]. The activity of the functioning photocatalyst is heavily dependent on the absorption of CO_2. Because of this, it is believed that the efficiency of CO_2 molecules may be improved by the application of surface engineering to the material. Cocatalysts also minimize the energy required for the first single electron's phase reduction process. Perovskite materials are being investigated intensively for

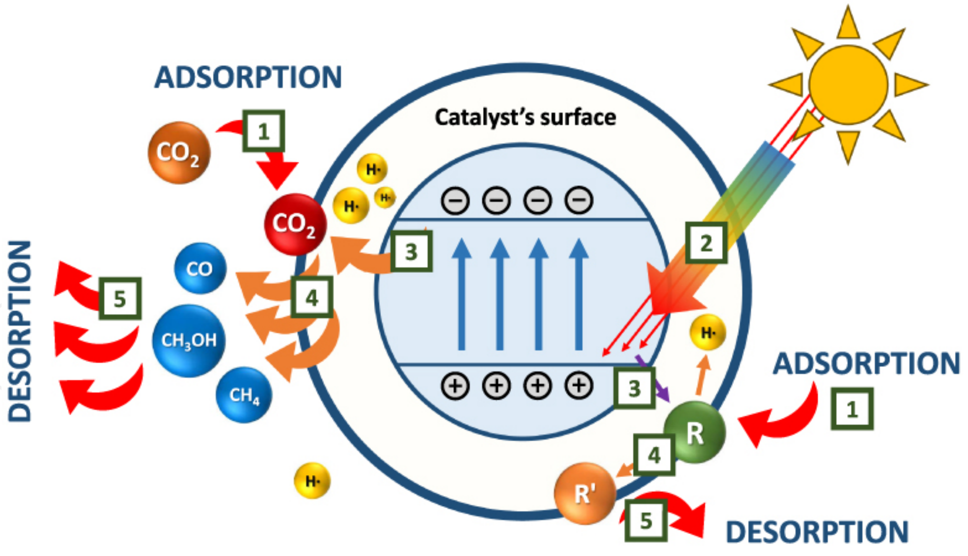

Figure 1. Photocatalytic CO_2 reduction process mechanism. Figure adapted from reference [38].

their potential use in photocatalytic CO_2 reductions [41]. An important challenge to overcome is that the carbon dioxide conversion efficiency is quite low in this process [42].

One of the most crucial things to keep in mind is that nature has only been able to achieve a 2% photosynthesis efficiency over the course of time. The process of photocatalytic CO_2 reduction is shown in Figure 1 [43]. As indicated in step 1 of the procedure, CO_2 molecules must appropriately adsorb just on the photocatalyst's surface in order for light photocatalytic activity to reduce them and thereby generate numerous useful compounds. Light is absorbed, and holes and electrons are formed in step 2 [44]. In step 3, photogenerated charges migrate to the catalyst's surface, while in step 4, they interact with the adsorbent species that have been attached. Step 5 concludes the process by removing the products formed from the surface, and this cycle is then repeated. Reduction potentials and the quantity of electrons involved in the reaction determine the products created in step 5. Photocatalytic CO_2 reduction may occur in both the gaseous and liquid states in the water medium when water vapor is present. Photocatalytic carbon dioxide reduction in the aqueous medium requires a photocatalyst with a valence band (VB) maximum lower than water's oxidation potential and a CB minimum greater than the carbon dioxide reduction potential to obtain the expected products [45]. Recombination of photoproduced carriers must be repressed to obtain successful photocatalytic changes, which may be done by paying attention to steps 2 and 3 of the process. In the oxidation half-reaction, the VB hole reacts with H_2O to produce O_2 molecules. They are used extensively in this process because they generate the H^+

ion required for the reduction reaction at CB by consuming the holes created in VB, which significantly speeds up photocatalytic CO_2 reduction. Most articles on photocatalytic carbon dioxide reduction omit the oxidation step, which is both useless and misleading [46]. It is also possible to use photocatalytic CO_2 reduction to compute the apparent quantum efficiency (AQE), allowing for more precise comparisons and assessments of the existing literature [47]. Most difficult and time-consuming molecules to synthesize is NH_3. Six electrons are required for the full reduction of a N_2 molecule to NH_3, rendering this process kinetically inoperable. Direct electron charge transfer (N_2/N_2–, −4.2 eV vs NHE) and proton-linked electron carrier transfer (N_2/N_2H, −3.2 eV vs NHE) are also impossible since a semiconductor lacks the required reduction potential. Thus, photocatalytic surface engineering and design are essential to the performance of this process, which assists in the weakening and activation of a N double bond while also providing a lower-energy alternative. Light irradiation also promotes the creation of holes and electrons, which subsequently migrate to the surface of the photocatalyst. If the functioning photocatalyst matches the reduction potential conditions, electrons and protons from water are transferred to the CB, where N_2 is reduced to NH_3 through a multistep transfer. Meanwhile, holes in the VB oxidize water molecules to generate O_2. Dissociated forms of hydrogen and nitrogen are produced by adding H_2 to a catalyst surface, where they are chemisorbed by H^+ and N_2 ions and dissociated or associated with adsorbed N_2 molecules. Finally, the catalyst surface absorbs the NH_3 that is created. There are two routes involved in this process, the dissociative and associative reduction pathways. Under ambient conditions, the dissociative route is often used in the Haber–Bosch process, which requires the breaking of nitrogen double bonds prior to the addition of H atoms [48]. The associative pathway, which makes use of alternative and distal circuits, does not need the breaking of nitrogen double bonds; hence N_2 fixation may take place under ambient conditions. Once the N–N link is severed in the associative route, the adsorbed N_2 N atoms are converted to NH_3 and subsequently desorb from the catalyst surface. Hydrogenation of nitrogen atoms takes place far away, and so does not interact with the catalyst directly. NH_3 molecules are formed from the residual nitrogen atom on the catalyst surface, which is hydrogenated. In contrast to the simple adsorption of N_2 on the catalyst surface, this process is challenging and requires a lot of effort. It is thus crucial to accomplish this reaction with surface engineering of the catalyst material, which is explained in depth in the next section. The formula that follows can be used to calculate the AQE for this process [49]:

$$\text{AQE} = [6 \times \text{no. of ammonia molecules evolved/no. of incident photons}] \times 100\%$$

In summary, photocatalysis may be a realistic solution to the current environmental and energy challenges. To make extensive use of these processes, it may be necessary

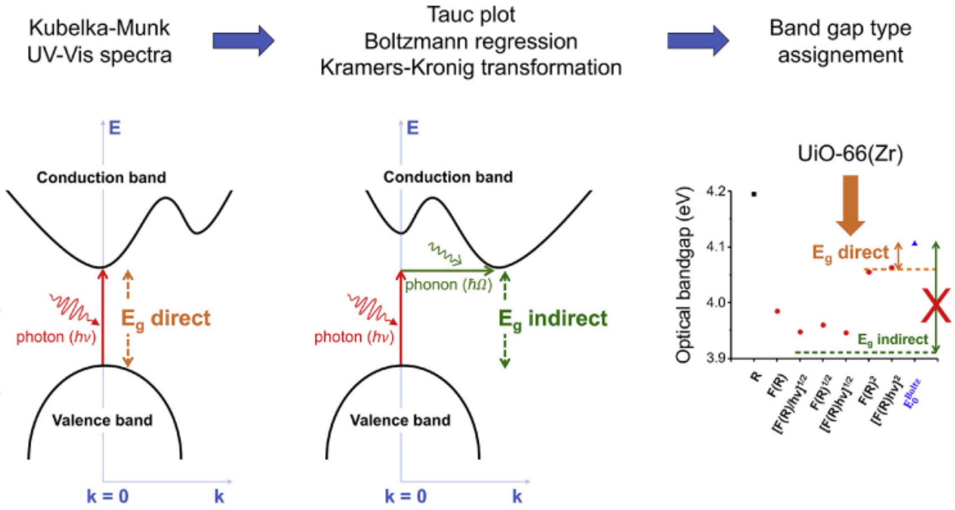

Figure 2. Three-band tailing versus band shifting in semiconductors materials [50].

to build interconnectivity between them. There is already a concern about rising carbon dioxide emissions due to the mineralization for large-scale pollutant degradation in the treatment of wastewater, and this must be handled with photocatalytic carbon dioxide reduction. Another way to eliminate hazardous emissions from the Haber–Bosch process while also saving energy is by large-scale photocatalytic N_2 fixation.

There are additional concerns about the ease of handling, transporting, and liquefaction of NH_3 as a H_2 storage carrier as shown in Figure 2. Using a sacrificial agent in photocatalysis, hydrogen expansion may be achieved on a large scale in polluted water owing to the partial utilization of the sacrificial reactant or carbon dioxide can be released if the sacrificial agent is mineralized. With this result in mind, it can be argued that photocatalysis may provide a long-term solution to resolve all of these concerns in a unified manner.

2.2. Photocatalytic pollutant degradation

Photocatalytic decomposition is a sophisticated method of oxidation that can be utilized to break down contaminants of high focus, difficulty, and limited biodegradability. Photocatalytic degradation uses light energy to degrade pollutants. Pollution compounds are oxidized and hydrolyzed through photon absorption in three electromagnetic regions: UV, visible (vis), and infrared (IR). When the photocatalytic substance is activated by vis/UV/IR light, the photosensitive electron migrates from the valence to the conduction band, resulting in photoinduced e–h pairs [51]. Photogenerated e–h pairs react with oxygen, water, and hydroxyl groups, resulting in reactive O_2 compounds such as superoxide radicals and hydroxyl radical anions. The radicals can degrade chronic contaminants either completely or partially. Photocatalysis activity has restrictions as they only exhibit in the UV range due to large bandgaps between the VB and CB. As a result, these materials demand high-energy illumination. Another difficulty is the rates of recombination of photogenerated electron/hole pairs and photocatalytic degradation. Incorporating carbon nanotubes (CNTs) is a viable technique to address difficulties and improve photocatalytic degradation. The CNT offers benefits in photocatalytic degradation, including improved transport characteristics and thermal endurance. They improve the separation of photogenerated e–h pairs, reducing recombination rates. The CNT's high specific surface area enhances pollutant attachment to photocatalytic reagents, leading to faster photocatalytic degradation. Using nanomaterials as substrates for modified CNTs can reduce aggregation, increase charge transfer in photocatalytic processes, and provide functional molecules that absorb pollutants [21]. One of the most appealing methods to lessen the contamination of water is the catalytic breakdown of contaminants in wastewater [52]. Adsorbents such as silica gel, metal-organic framework, activated charcoal, and so on need to fulfill several conditions to recover their absorption, making this technique more dependable. Aside from these environmental concerns, solvents and chemicals used in recycling may be costly and harmful to the environment. Degradation of organic pollutants by photocatalytic degradation is faster because the reactive species produced during light catalysis attack and destroy the pollutant molecules more rapidly [53]. There are several instances where photocatalytic degradation of organic pollutants leads to the production of low-molecular-weight or mineralized compounds. With its self-cleaning surface and heterogeneous nature, the catalyst is also straightforward to recycle since all reactions take place on the catalyst's surface, followed by the desorption of products. It is therefore an environmentally friendly and green solution to water pollution issues that this method provides [54–57]. A deterioration process, on the other hand, might result in a product that is not necessarily ecologically sound. The cleavage of dye molecules into smaller pieces may cause dye discoloration during this procedure as well. It is thus impossible to estimate photocatalytic effectiveness by studying absorption spectra of target dyes alone. It is necessary to offer additional data such as total organic carbon and chemical oxygen demand to verify mineralization [58]. In order to produce active species in response to light irradiation, water must be present as a reaction medium. For photoinduced charges to react with adsorbent species before the recombination process, they must first reach the catalyst surface. Adsorbed oxygen and H_2O molecules in the functioning photocatalyst combine with light-generated charges to form the active species, which is entirely reliant on the VB and CB edges. A mineralization process is expected to take place as a consequence of the highly reactive nature of these active species. To complete the degradation process, additional pollutants are adsorbed onto the surface of the catalyst, where degradation products are desorbed and then readsorbed. Furthermore, the recombination of photoproduced charges must be inhibited in order for these species to develop effectively and have significant photocatalytic activity [59, 60]. This makes perovskite oxide (ABX_3) based materials potential candidates for the photocatalytic degradation of a broad variety of organic pollutants such as dyes, herbicides, fungicides, pharmaceutical waste, and the like.

3. Advancements in photocatalyst immobilization and supports

There has now been a shift in focus on assembling perovskite catalysts, which reveals their structure and evaluates the influence of photo-oxidation on high-resolution reactions. Perovskite catalysts provide substantial area-to-volume ratio and active charge separation and attach themselves to visible surfaces [61]. The dazzling opaqueness of these nanoscale perovskite catalysts has been found to have increased drainage capacity compared with bulk perovskite catalysts [62]. A critical challenge in big water treatment systems is the size and shape of nanoscale perovskite catalysts even though the physical and chemical qualities have improved dramatically. The perovskite slurry photocatalyst is now constrained by technical obstacles. With regard to the utilization of direct sunlight, this new perovskite catalyst with dopants will be briefly presented. Degussa P-25 TiO_2 catalysts have been used extensively in water treatment research to date. The photoactivity of the catalyst has been used as a reference standard in numerous medical scenarios. Small particles of Degussa P-25 perovskite are widely used in a muddy season in solar cells. The use of perovskite as a catalytic system and potential technical solutions to challenges are currently being studied. In general, a larger volumetric reactive oxygen species (ROS) production is connected with the catalyst for suspension [63] as compared to the total number of active sites.

To construct catalysts on an inert substrate, the number of active sites is reduced while mass-transfer limits are increased. Immobilization of catalysts makes them more difficult to function [65] since an incoming photon may not reach the whole image processing region. Consequently, the slurry type employed in perovskite catalyst applications is frequently preferred over other types. There will be one more phase in perovskite slurry systems once the catalysts are added. In order to prevent the loss of the catalyst and the creation of new perovskite contaminants in clean water, this separation step is essential. Regeneration of catalysts may be accomplished by a variety of methods, including mixing with sedimentation, using a cross-flow filter, and using various membrane filters [66]. pH of materials being adjusted near the isoelectric coagulation area, 3% of the catalyst particles undergoing the hybrid microfiltration (MF) process may return for reuse.

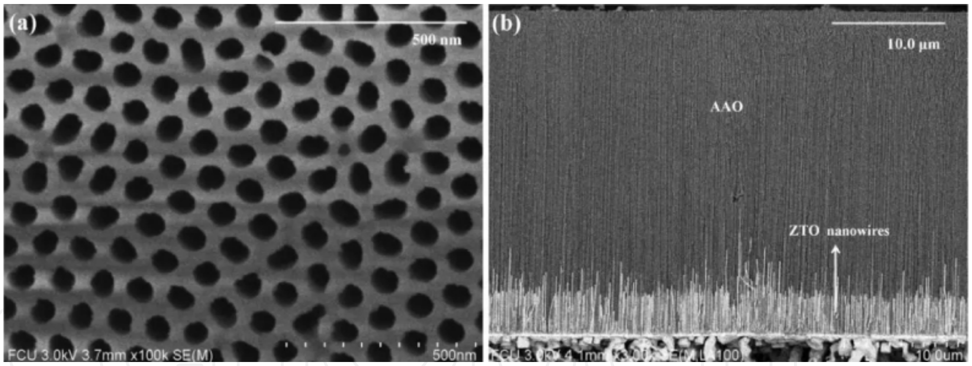

Figure 3. FE-SEM images of perovskite nanowire membranes showing bundle formation. Figure adapted from reference [64].

Some substantial performance issues with perovskite slurry persist even after we have covered the membrane procedure. Several studies have demonstrated that using microns shortens the fixation of the catalyst, improves local interaction with contaminants, and prevents membrane contamination or pore obstruction in the nearby environment. Immobilizers include, for example, activated carbon, mesoporous clay, threads, and the membrane itself [67, 68]. Many forms of renewable energy that may be produced using either membrane or slurry reactors, or even both. Clean water may flow continuously without losing photoactive particles if photocatalytic reactions occur more often in the membrane, as shown by the current study. Photocatalytic membranes (PMs) may be created using a variety of materials and techniques. There are several examples of this, including the TiO_2/Al_2O_3 combination fluid [69]. Phosphorus-containing polymer membranes are confined inside the membrane structure during the membrane formation process of perovskite or dots. As a potential material for both inorganic and organic ceramic membranes, perovskite has also been studied in depth. The many forms of PMs employed in water treatment are shown in Figure 3 [70]. There are several technical difficulties that have been observed with PMs, including membrane structural degradation, restricted photocatalytic activity, and loss of the perovskite layer. A slurry–membrane hybrid may be constructed to alleviate difficulties with perovskite membrane coating by using a membrane without adding a perovskite layer. Perovskite's photocatalytic reaction occurs below ambient operating conditions; hence the photoactivity of photonic activation catalysts is often confined to a small wavelength range. A high and UV spectrophotometer is required for catalyst activation, and it comes at a high cost. Another option is to use a large quantity of external solar radiation to improve the efficiency of the catalyst. Composite photocatalysts incorporating CNT, fine metal ions or metal inclusion, transition metal, and nonmetal doping [71, 72] have been created to expand the image response of perovskite catalysts for the solar spectrum. Material engineering approaches may be utilized to monitor the reaction level of a photocatalytic process by changing the structure of the catalyst. Various methods may be used to increase the photoactivity of catalysts. Receptive electrons may promote and completely prevent electron–hole pair reunion when they are present. When exposed to direct sunlight, the scanning performance of converted perovskite catalysts improves. The CNT-linked CNT was able to show a possible increase in electron pairs by capturing electrons inside its structure. Dye molecules that become excited in sunlight may donate extra electrons to the CB for the creation of electron–hole pairs [71]. Solar irradiation is often used to activate dyes such as methylene blue and azure, as well as erythrosine, rhodamine, and crystal violet.

4. Photocatalytic reactor configuration

A photocatalytic reactor may be divided into two groups based on the photocatalyst condition used: (1) fixed photocatalytic particles and (2) reactors with fixed photocatalytic particles in a continuous carrier [73]. It is possible to use many types of photocatalytic water treatment reactors, such as the cascade photoreactor and the downflow contactor reactor. Photocatalyst particles may be accessed continuously in the second design, but the first needs an extra subdivision unit to do so. Photocatalytic reactors must have a general bright catalyst region with a unit volume and light dispersion inside the reactor, according to [74]. Because of the mass-transfer limitations across a continuous layer of photosynthetic materials, the reactor typically generates a photocatalyst surface area equal to the volume of the reactor. However, the bed arrangement may vary. The distribution of photon light in reactors must be established either directly or indirectly. Photocatalysts with "direct photon use" transfer pictures directly rather than using a parabolic light deflector system.

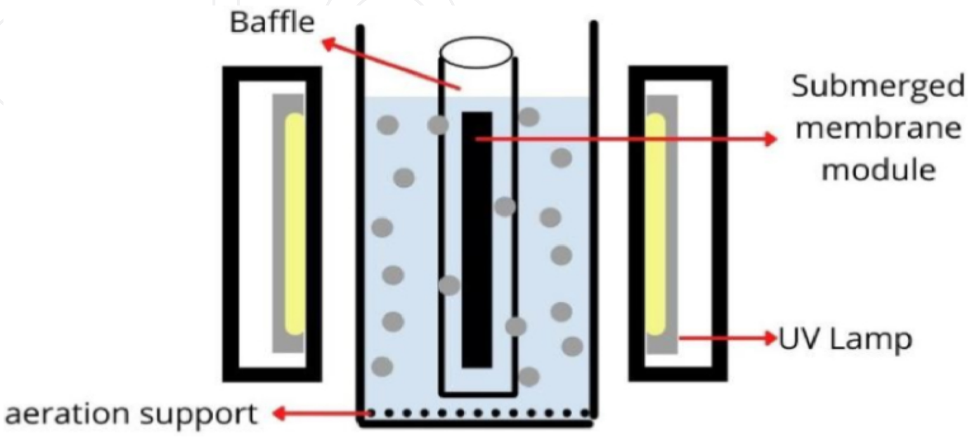

Figure 4. Schematic of submerged photocatalytic membrane reactor [75].

It is essential to ensure that the reactor's photon flux is evenly distributed throughout the reactor by positioning the source of light precisely. These photoreactors are no longer extensively employed because of their specific configuration and high operating costs. In order to achieve low pressures, a large reactor volume, and effective catalyst blending and dispersion, this kind of reactor must be designed precisely. It was formerly the usual practice to use a slurry photocatalytic reactor because of its huge photocatalyst surface area per unit volume and the simplicity with which it could be replaced. A photocatalyst particle may be separated using settling tanks or an external cross-flow filtering device to enable continuous operation of the slurry reactor. The use of hybrid photocatalysis membrane approaches to resolve the separation of photocatalyst particles after treatment is a potential solution. This hybrid method eliminates the need for any flocculation, coagulation, or sedimentation separating catalyst particles in the filtered water stream. Additionally, you may save on the size of the process installation and the site area needed. We often refer to the hybrid system as "photocatalytic membrane reactors" when we speak about these devices (PMRs).

A membrane filtering unit may be positioned in a separate location from the photocatalytic reactor because of the hybrid system's design. There were two reaction zones: a UV-slurry perovskite zone and a submerged membrane module that was separated by a moving barrier. A light feed tank with photocatalyst suspensions may also be used to manufacture these PMRs [76]. It is possible to preconfigure photocatalysts to be inserted into membranes or dispersed in wastewater. It is possible to perform (a) steps to awaken sensitization in the presence of organic adsorbed electron acceptors, which include (b) ion-doped perovskite band structure and (c) ion-implanted perovskite (physically implanted without losing any photocatalyst particle). Before passing through a hybrid membrane system for filtration, this permits clean water to reach the previously determined level. Static photocatalyst particles are supported by the membrane module, which functions as a barrier to distinct organic molecules in the wastewater. Photocatalysts and organic particles are also kept out by the membrane. Simple PMRs are molecules or intermediates that will be removed from the process. In PMRs with photocatalysts that cannot migrate, photocatalytic reactions take place on the membrane structures. Perhaps, hidden amid its cracks and crevices? There are three types of PMs that may be used in accordance with colloidal size and water quality requirements: MF, ultrafiltration (UF), and NF. Both UF and NF have a direct effect on the particle size width at this stage—0.1 eV, 5 mm colloidal size. The photo-oxidation efficiency of pollutants may be improved by using an inactive PM rather than PMRs with the fixed catalyst particle. However, it has been shown that their direct interaction with hydroxyl radicals and UV-blocking photocatalyst particles causes issues and damages the membrane structure [77]. Thus, the membrane hybridization structure with a suspended photocatalyst appears to be an excellent option. It has been extensively documented that this PMR configuration degrades the humic water phase; phenol, bisphenol, and 4-nitrophenol and 4-chlorophenol; water vapor; para chlorobenzoate; and river water as well as dyes and fulvic acid [75, 78].

5. Water splitting or photocatalytic water treatment processes

Energy and environmental issues are major problems across the world. Clean energy solutions must be developed if we are to overcome the challenges we face. In the system, hydrogen will play an important role due to its ability to be utilized in fuel cells. There are several uses of hydrogen in the chemical industry. The creation of ammonia, for example, requires the use of large amounts of hydrogen. Currently, the majority of hydrogen is created by converting steam from solid fuels like natural gas into fuel.

$$CO + H_2O \rightarrow CO_2 + H_2 \tag{1}$$

Since new testing equipment is currently being developed, the possible application of photocatalytic water purification systems in the industry is now being examined. CO_2 is released as a result of the use of mineral oil in this procedure. Solar energy, for example, may be used to produce hydrogen in a way that is environmentally friendly and efficient. As a consequence, water's ability to produce solar hydrogen has been enhanced. Hydrogen from the sun may be generated in many different ways, for example, solar-powered water electrolysis, hydroelectric power production, conversion of biomass into energy, photocatalytic or PEC separation of water (synthetic photosynthesis), etc. Testing facilities have been established to obtain data on the effectiveness of medicines, volume directed to site needs, electricity consumption, and carbon emissions from the manufacturing process. Research on photocatalysis and photo-Fenton at INETI in Portugal and PSA in Spain has yielded a significant amount of data for technical study. Both of these institutions are well known for their experimental photovoltaic (PV) systems. Integrated parabolic collectors (aperture area A 4.16 m^2) exposed to the sun, a reservoir drum, a recycling pump, and connecting tubes are included in both plants' batch modes. These plants are described in further detail in the literature [79]. For evaluating these photocatalytic systems as a new water/waste technology treatment, life cycle testing should be investigated based on current data that is already accessible. An extensive number of generally accepted life cycle assessments (LCAs) account for not only the natural effects of water photocatalytic treatment but also the technology's viability and cost [80]. According to experts, ROS-based oxidation may also be used for applications that need high energy consumption and high utilization of reactants. Consider the photocatalytic treatment of water as a whole; a thorough LCA based on meaningful technical knowledge should be carried out. Heterogeneous photocatalysis and other advanced oxidation processes were included in simplified LCA-based evidence in the laboratory. However, they found that in their LCA study, interpreting limited laboratory data might lead to this incomplete conclusion. LCA may be used to identify and reduce waste and environmental repercussions, and discover opportunities for improvement across the life cycle of goods, processes, or activities with strength scales and materials [81]. This is the best LCA decision-making technique since it encompasses all loads and effects and focuses on both production and the waste created.

Toxic chemicals can be destroyed at a noncorrosive level in accordance with water quality standards. Investigators [82] conducted an LCA study on two prototypes at INETI and PSA facilities that treat 1.0 m^3 of methylphenyl glycerin. The assessment of raw materials and energy will be aided by yet another set of technically competent estimates. Global warming, depletion of the ozone layer, contamination of clean water affecting human health, photochemical oxidation formation, nonrenewable energy use, eutrophication, acidification, and land use energy were all considered in the study. Photocatalytic technology is used to estimate the large-scale LCA impact of water. While photocatalysis wastewater treatment systems have low eutrophication power, they need substantial site area and energy consumption, according to the findings of the LCA. The parabolic construction material collecting equipment as well as the high pumping capacity required are technical hurdles that are a direct outcome of the system's pollution. There is, however, no way to directly compare the findings of the effect categories as they are reported in a different measurement unit. These difficulties stem from the weak photoactivity of catalysts used in sunlight, which is especially troublesome from an engineering perspective. Engineering and research should be carried out to address these technological hurdles in order to facilitate the active marketing of technologies in a commercial context. For simplicity, photo/catalyst powder is used in water-separation operations as shown in Figure 4. Photocatalyst particles scattered over a pool of water make hydrogen readily available when exposed to sunlight. The necessity to separate H_2 from O_2 has no effect on photocatalytic water separation. The Z-scheme photocatalyst system, on the other hand, will be able to solve the issue. Additionally, the ease of use of solar water separation in powdered photocatalyst systems will lead to increased utilization. The long-term sustainability of green chemistry and the settlement of environmental and energy concerns that lead to energy transformation will benefit from photocatalytic water separation. The Gibbs free energy is significantly altered when photon energy is converted to chemical energy through water separation. This mechanism is similar to photosynthesis in green plants. Synthetic photosynthesis is a term used to describe photocatalytic water separation, an interesting and challenging area of chemistry.

Decomposition in the photocatalytic process is similar to that of an organic substance, wherein oxygen molecules are used to convert free energy into chemical energy, as in Gibbs' idea of free energy conversion. The photochemical nature of this degradation process has led to a great deal of research into it [81].

'The initial step (1) The initial step (1) is the absorption of a photon to form electron–hole pairs. Many heterogeneous photocatalysts' semiconductor properties have been identified. Semiconducting devices are the next step in the photocatalytic process, as seen in Figure 5. In semiconductors, the conductor and the VB are separated by the correct width of bandgap energy. When the incoming light intensity exceeds the bandgap, electrons and holes are generated in the operating band and the valence band, respectively [83]. As a general rule, water molecules are reduced by the electron to H_2 and oxidized by holes to O_2 for water separation. The bandgap width performances and valency of semiconductor photocatalysts are critical features. There is a good chance that the low bandwidth redox power of H^+/H_2 will be much larger than the redox power of O_2/H_2O (0 V vs NHE) (1.23 V). Consequently, the water-separation band's fundamental gap is 1.23 eV and its brightness is around 1100 nm.

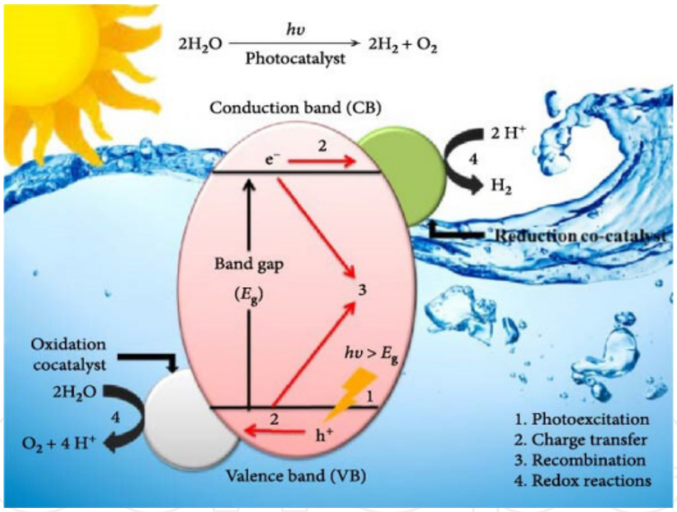

Figure 5. Main processes in photocatalytic water splitting [84].

Network-generated system charges and migrations are categorized in the second step (2) of Figure 5. As seen in Figure 5, the crystal structure and particle size all have a major influence on this step. The degree of distortion is small provided the crystal result is excellent. Since errors serve as places where generated electrons may be captured and reconnected, photocatalytic activity is decreased. Reduced recurrence occurs when the distance electrons and holes must travel to reach a higher reaction site decreases. The third step (Figure 5) involves the reaction of the excess chemicals. This stage is all about the value and nature of the region above (the active area) (upper area). No matter how strong the H_2O separation is, if there are not enough active redox reaction sites, electrons and holes will have to come back together [85]. To activate H_2 evolution sites, metal-oxide photocatalyst cocatalysts such as Pt, RuO_2, and NiO are typically used since their CB levels are high enough to reduce water and produce H_2 on their own. For O_2 formation, an active site for 4-electron oxidation of water is needed. Because the VB is deep enough to oxidize water to form O_2, cocatalysts are typically not needed for oxide photocatalysts [86]. This is a defining point of heterogeneous photocatalysts that varies from comparable photocatalysts in that the appearance of O_2 and 4-electron oxidation of H_2O is a hard process. The reverse reaction to water creation via interaction between the modified O_2, H_2, and the medium proceeds readily owing to the increasing reaction. Therefore, weak rear reaction structures are necessary in the presence of the photocatalyst and cocatalyst. Many photocatalysts are also composed of phosphors, solar cells, and dielectrics. However, an essential distinction between photocatalysts and other substances is that chemical processes are involved in the photocatalytic process, but not in other apparent structures. Only if the three processes depicted in Figure 5 are performed concurrently, photocatalytic capabilities may be achieved. Consequently, the surface structure, bulk, and energy structure of photocatalysts all need to be of sufficiently high quality. Because of this, it is no surprise that the most efficient chemicals are photocatalysts. For future problem-solving, scientists and engineers are pursuing solar water splitting, which includes photocatalytic processes [87].

5.1. Photocatalytic reactions

5.1.1. Photochemical reactions

Photochemistry is a discipline of physics/chemistry that studies the rates and processes of reactions that occur when reactants are exposed to light radiations. The photochemical reaction is actually a thermal response of the molecule's electrically excited state, whereas the dark reaction is a thermodynamic reaction of its neutral state. The process of a photoresponse ought to ideally include a full definition of the major events as defined by the categorization of photochemical reaction paths. Quantum production, or unit constants, of all important photochemical and photophysical reactions, provides data on the shape and destiny of any reactive intermediary molecules, as well as their periods of existence and reactivities [88]. A catalyst, an electron donor, and an absorber of visible light are the three main components that comprise heterogeneous photochemical water splitting. The core ideas of photochemical and photoelectrochemical systems are the same; however, the configuration is different. The water-splitting mechanism occurs at the semiconductor–electrolyte interface in photochemical reactions (Figure 6). At the semiconductor–liquid junction, the requisite voltage for water splitting is produced. To prevent corrosion, the semiconductor must be stable in the electrolyte whichever direction the semiconductor’s band edge is. As was discussed earlier, they may be involved in the generation of O, H_2, or entire water splitting [89].

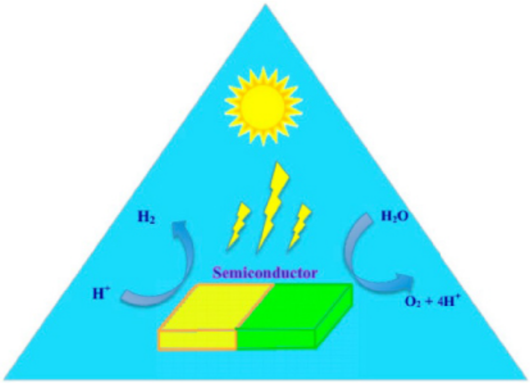

Figure 6. Schematic representation of water splitting by photochemistry [90].

5.1.2. Photoelectrochemical reaction

During PEC WS, a photocatalyst (a semiconductor) is exposed to UV light with energy greater than or equal to the semiconductor’s bandgap (Figure 7). Charge separation occurs in the VB and CB after the photocatalyst absorbs light energy. The photoexcited electron is positioned in the CB while holes are produced in the VB. Photoexcited electrons reduce absorbed H^+ to H_2 in the CB as the holes oxidize water at the CB’s surface. Semiconductors are utilized as a photocathode or anode in PEC WS depending on which reactions are favored. The electrolyte and redox pair must be in close proximity for PEC WS to be successful. During PEC WS, two different electrodes are used to conduct the whole process. The voltage necessary for water splitting can be supplied by lighting the anode or cathode in this manner [91].

5.2. Hydrogen production from water

Semiconductor photocatalysis relies heavily on the electrical structure of the semiconductor itself. As opposed to a conductor, semiconductors are made up of VB and CB. The energy differential between these two levels is known as the bandgap (Eg). A photon that has energy more than or equal to the bandgap level excites semiconductors, and this causes the electron to acquire energy, moving it from the CB to the VB. The electron and hole are both in the VB if there is no excitation. Photogenerated holes and electrons may recombine in the semiconductor bulk or on its surface in a very short period of time, releasing energy from heat or photons [92]. The reactant adsorbed by the semiconductor may be reduced and oxidized by

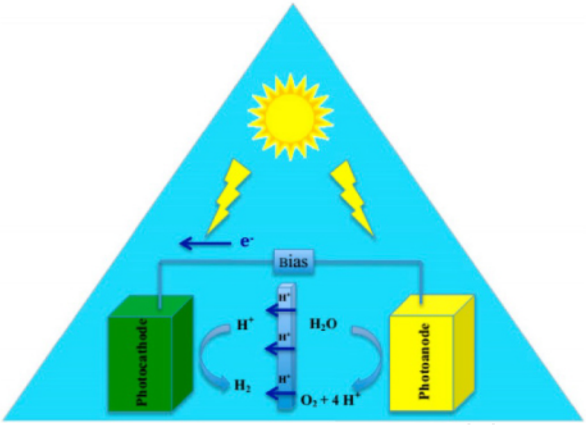

Figure 7. Schematic representation of photoelectrochemical water splitting [90].

electrons and holes that travel to the surface of the semiconductor without recombination. There are two fundamental reactions that occur in photocatalytic hydrogen generation and water/air purification processes: oxidation and reduction. A higher reactive surface area provided by nanosized semiconductors improves both surface adsorption and photocatalytic reactions. Oxygen generation from water via photocatalysis requires that the CB and VB levels be more negative than the hydrogen production and water oxidation levels, respectively [93]. All kinds of semiconductors that fulfill the above parameters may potentially be utilized as photocatalysts. Water splitting will not work with most semiconductors that produce photocorrosion, such as SiC and CdS.

Because of its high chemical stability, catalytic activity, and extended lifespan of electron/hole pairs, TiO_2 is the most widely used photocatalyst. Due to the following variables, the energy conversion efficiency of TiO_2 photocatalytic water splitting from sunlight to hydrogen is presently low: (1) recombination of electron/hole pairs produced by photons: CB electrons may swiftly interact with VB holes, releasing energy as waste heat or photons [94–96]; (2) rapid backward reaction: since the conversion of H_2O into carbon and oxygen requires energy, the backward reaction (recombination of carbon and oxygen into water) is rapid. Because TiO_2 has a bandgap of roughly 3.6 eV, only UV light can be utilized to create hydrogen. Being unable to use visible light reduces the efficiency of solar photocatalyst hydrogen synthesis since visible light contributes to about 50% of solar radiation energy (E) whereas UV light only makes up about 4%. Continuous attempts have been made to increase photocatalytic activity and improve visible light sensitivity in order to get around the issues mentioned above and make solar photocatalytic H_2 generation practical. Electron donors (hole scavengers), metal ion doping, noble metal loading, carbonate salt, and anion have all been investigated, with some of them showing to be effective in increasing hydrogen generation. Chemical additives and photocatalyst modification methods are the two main categories for the above-mentioned procedures that impact H_2 generation.

5.3. Water quality and removal of inorganic compounds from water

In a full-scale water treatment facility, a number of technological problems must be overcome. The water quality in the influents of treatment plants may fluctuate over time. This section will look at the implications of TiO_2 photocatalytic processes for the treatment of diverse H_2O sources. This provides a better understanding of how numerous key water quality factors influence the applicability of advanced TiO_2 photocatalytic procedures.

Turbidity: Turbidity is the term used to describe a water body's high concentration of insoluble particles. Such insoluble particulate contaminants can alter optical characteristics and further impede the entry of UV light by significantly absorbing and scattering it, which is especially detrimental to the TiO_2 photocatalysis-based approach [97]. As a consequence, the projected use of TiO_2 loading, UV penetration route, and light intensity will all vary. Furthermore, excessive levels of turbidity may diminish the efficiency of photodisinfection and photomineralization of pollutants in water by reducing light penetration, leading contaminants to escape the treatment [98]. Target pollutants will also be protected from oxidation by suspended solids. The nonfiltered residue that remains on the filter media after filtration is referred to as suspended solids in this case. All of these variables lead to a decrease in overall photocatalytic efficiency in the treatment of water. The turbidity of the target water must be maintained below 5 nephelometric turbidity units (NTU) for optimal UV light consumption and photocatalytic reaction. The authors of [57] discovered that water turbidity of more than 30 NTU reduces the photocatalytic disinfection rate. The 5 NTU limit is arbitrary, and it is decided by both the incoming water and the treatment levels required. Traditional treatment procedures such as screening, sedimentation, filtration, coagulation, and flocculation might be employed initially to minimize turbidity since TiO_2 photocatalytic reactions are retrofitted to advanced wastewater treatment stages. 1 mg of specific-size silica suspension per liter of particular size silica suspension that may be generated for laboratory analysis. By using an electromagnetic detector to measure the intensity of scattered light, turbidity standards can be adjusted. Inorganic ions are predicted to be present in the water undergoing TiO_2 photocatalytic treatment. To functionalize a TiO_2 water treatment approach, a fundamental knowledge of the effects of organic ions on photocatalytic performance is necessary. According to [99], photocatalyst deactivation is often seen when a photocatalyst is utilized in either a slurry or a bed configuration setup to treat real fluids containing various inorganic ions. The inorganic ions on the TiO_2 semiconductors serve as a powerful inhibitor. To guarantee that the TiO_2-based treatment process functions as effectively as possible, the presence of these inorganic ions, as well as their permissible levels, in the photocatalytic performances of TiO_2 in water treatment, must be recognized. This information may be used to modify fouling prevention using photocatalysts and inorganic ion regeneration methods. There have been several studies on the effects of different inorganic anions or cations on TiO_2 photomineralization and photodisinfection processes [100]. However, the bulk of these studies have focused on how organic ion variations impact the rate of photocatalytic reactions using an organic molecule surrogate model. The surrogate model organic compound may be biased toward photocatalytic activity due to its underlying chemical characteristics and major component groups that make up the molecule. Model molecules with electron-withdrawing or electron-donating groups, for example, will participate in the breakdown process to varying degree [101]. Due to the zwitterionic character of the TiO_2 particle, the operational pH may have a significant impact on the particular inhibition of inorganic ions on the structure. The influence of the chemical characteristics of the organic model employed and the operational pH in the photocatalytic reactor on the inhibition of various inorganic ions used in the photocatalytic treatment of water, nevertheless, has not received much attention. The effects of inorganic cations and anions (such as Cl, NO_3, ClO_4, HCO_3, SO_4, HPO_4, and PO_4) on photocatalytic water treatment have been investigated [100]. According to these investigations, Cu_2, Fe_2, Al_3, Cl, and PO_4 may inhibit photomineralization reaction rates at certain concentrations, but Ca_2, Mg_2, and Zn_2 may have the reverse effect. This is due to the fact that Ca_2, Mg_2, and Zn_2 are in their highest oxidation states, making them incapable of inhibiting the photocatalytic process. Fe_2 may catalyze both the photo-Fenton and Fenton reactions. Fe_2 fouls the photocatalyst surface by generating $Fe(OH)_3$, while PO_3^4 remains heavily adsorbed onto the TiO_2 surface in the usual pH range, limiting its photoactivity [102]. NO_3, SO_2^4, ClO_4, and HCO_3 have been reported to diminish photocatalyst surface activity in certain investigations but not in others. Photodisinfection is harmed by both SO_4 and NO_3 [103]. Cu_2 may increase photocatalytic activity by 0.1 mM, while greater doses slow down the reaction rate. NH_4 and principally NO_3 are produced when nitrogen-containing substances are mineralized. The proportion of ammonium ions is mostly governed by the degree of nitrogen oxidation at the start of the irradiation period. Sulfur atoms in pollutants are converted to sulfate ions in the body. Cl has no effect on the photocatalytic breakdown of trichloroethylene at concentrations up to 3.0 mM. Oxyanion oxidants such as ClO_3, ClO_2, IO_4, S_2O_8, and BrO_3 increase photoreactivity by scavenging CB electrons and limiting charge-carrier recombination [104]. The addition of salts is known to impair colloidal stability as the screening action becomes more pronounced. Surface charge neutralization and double-layer compression that follow decrease surface contacts between contaminants and catalysts, increasing mass-transfer limits. Other inorganic ions have an impact on photodegradation rates, such as SO_4 in a TiO_2-coated glass spiral reactor, which may quadruple the rate of disappearance of the insecticide monocrotophos. Mn_2 improves photoactivity by boosting electron–hole pairs while simultaneously limiting recombination. The fouling impact of inorganic ions on TiO_2 photoactivity has been proposed via many mechanisms. These mechanisms include UV screening, photon competition, precipitate deposition on the surface, competitive adsorption to the surface-active site and elemental metal, radical and hole scavenging, and direct interaction with the photocatalyst. The NO_3 ion has been demonstrated to UV-screen rather than block the TiO_2 surface of the photocatalyst [105]. The constant displacement of hydroxide ions from the TiO_2 surface due to competition for the surface-active site reduces radical generation even further. Quantum yield is reduced because inorganic ions compete directly for light photons (lowered number of photons entering the reactor). A similar drop in efficiency is seen in photonics when precipitates are produced and deposited on the TiO_2 surface, reducing the availability of both photons and organic molecules. The ultimate inorganic anion that has been discovered to scavenge both radicals and holes is Cl. HCO_3, SO_4, and PO_4 proposed a hole and hydroxyl radical scavenging mechanism for limiting photocatalysis. Chlorine's inhibition of TiO_2 photocatalysis is explained by a preference for adsorbed displacement over surface-bound OH ions. The substituted Cl enhances electron–hole pair recombination while reducing the quantity of OH ions accessible on the TiO_2 surface. In solution, Cl ions, like other chlorinated compounds, are quickly released. This characteristic might be beneficial in a technique that includes a biological depuration mechanism as well as photocatalysis, which is generally inefficient for chlorinated compounds [106, 107]. The adsorption of amino acids onto TiO_2 catalysts has been shown to be inhibited by other ions, such as PO_4, while CO_3 along with other ionic species attack organisms and further limit efficiency when they interact with the OH radical. As a result, an essential component of water treated by TiO_2 photocatalysis inorganic ions.

6. Organic photovoltaics

In most biological semiconductors, the Coulomb-bound exciton is the principal source of excitation. Photovoltaic cells have poor power conversion and external quantum efficiency (EQE) or photon-to-current conversion efficiency since they are made up of single organic semiconductors. A high EQE is not necessary for excellent PV power conversion, but it is a requirement. The EQEs of inorganic photovoltaic cells are often close to 100%. In organic photovoltaic (OPV) devices with a single layer of polymeric semiconductor, EQEs are generally less than 1%. The solution came about in 1995 when various groups independently claimed that the EQE could be increased by several orders of magnitude by combining two common favorable factors for negative and positive charges [108]. The difference in electron affinities acts as a driving force, causing the exciton formed by the picture in the visual connection between two objects. The optical connection is distributed across the device by linking nanostructured components (approximately 10 nm). As a consequence, if the charge transfer is much quicker than competing reconnection channels, whether with or without radiation, all excitons produced by the picture are likely to locate a visible connector and split before reassembling. The notion of combining p-type semiconductors with n-type semiconductors has gained momentum under the label 'bulk heterojunction composite'. The EQE represents the proportion of light excitations that survive both transit and cost-sharing methods. The EQE has improved from 29% to 50% [109] with the application of the heterojunction (HJ) idea in general, with an EQE of 80% being recently reported. These very high numbers were obtained by combining composite polymers with fullerenes. As a renewable energy source, the solution might be treated similarly to polymeric PVs. Unfortunately, the general energy conversion efficiency is low under typical sunlight conditions. Only a 3.5% performance has been recorded so far, and a large 5% projection was recently surpassed [110]. Despite the high EQE of live absorbers in the sun spectrum, one of the primary reasons for this. Even though the sun's photon mass is 700 nm, the majority of current biological semiconductors absorb visual irritants. Another difficulty is that organic compounds have limited internal stability: when electrons have high orbital energy, instances that resist binding and compound degradation become more prevalent. In the case of n-type semiconductors, this is especially true. Finally, for collecting light on the composite's PV system, efficient cost transportation and separation are necessary. The power band of the two objects should first be relaxed to ensure charging following optical excitation. This needs a complex morphology between the two substances, with nanometer-scale nodes preventing arrangements and 100-nm-scale systemic circuits providing effective transport pathways. Creating the most space-efficient HJ between the receiver and donor objects is one way to get around the exciton diffusion bottleneck. By merging multiple circuits in this case, a circuit is created in which photons may be extracted across a greater distance, resulting in the generation of all excitons inside the donor–acceptor (DA) interface distribution length, allowing for image-charged charge transfer. A polymer and fullerene mixture was used to create a flexible network that spans the device in the first demonstration of a mass HJ. In comparison to a basic planar structure, this strategy has resulted in considerable increases in power conversion efficiency (PCE) [111]. Building HJ-based molecular-weight is very challenging because phase separation must occur on a solid surface rather than in a liquid phase as it happens with polymers. As seen in the pairing of the DA, CuPc, and PTCBI archetype pairs [112], simply mixing the materials with variations of the donor molecule and the receiving source on the substrate can result in a significant reduction in network traffic. Movement (and, as a result, an increase in resistance to a series of cells) results in the formation of molecular planes. CuPc and PTCBI create structured stacks in pure thin films, which enables charge transfer to a dispersed electron system at the packing destination. When the stacks are placed in a mixer, the distribution and charging are disrupted during passage to the electrodes. As a consequence, a mixed-layer device often has poor conversion power (0.1%). A thin film, on the other hand, is not a sculptural piece. As a consequence, phase separation at HJ bonding may be achieved by subjecting the mixture to high temperatures. Following the CuPc/PTCBI cell, Peumans and colleagues demonstrated that compressing a double layer of HJ at 2000 °C for 10 minutes can result in the film's inner light in the mass. For the past several years, OPV cells have been a prominent focus of study due to their potential to reduce energy consumption and the environmental problems caused by growing fossil fuel burning. Many efforts have been made to better understand PV technology, including the development of chemical motif elements and device structure design, which has resulted in significant increases in OPV cell efficiency conversion from 3% to over 15%. This short research summarizes the high degree of upgrade and advancement made by OPV cells in recent years. Based on a few new enhanced ways of properly detecting electron–hole pairs in the femtosecond state, a theoretical framework is addressed for applying a comprehensive image of the power harvesting equipment necessary to charge network firm development, especially in bulk OPV cells with multiple HJs. Unique OPV device architecture designs, including outward geometric modification and inner ornamentation, were later introduced. Alternatives to dynamics and thermotics, as well as other approaches for boosting the efficiency of OPV cells, are considered. Photovoltaic technologies, which allow for direct solar production, are expected to play a significant role in nature and provide a long-term solution to the world's energy problem. Photovoltaic cells' future success will hinge on the advancement of cell and material research design approaches that improve device performance and accuracy while lowering manufacturing, installation, and operating costs [113]. Traditional PV technology, however, has not been able to effectively replace grid power because of high production costs and environmental issues, and PV-generated electricity accounts for less than 0.1% of total energy output worldwide. Organic photovoltaic cells and organic light-emitting devices (OLEDs) have sparked interest in recent decades because of their variety, low-cost method, and high energy efficiency [114]. By building materials that are both flexible and adaptable, OLED displays and solid-state lighting have already been marketed, but OPV has moved from a trendy idea with a PCE of less than 1% to a market-ready product with a PCE of more than 10%. Photovoltaic distinction between inorganic and natural PV cells is the relevance of surface contact processes. A fundamental purpose of almost all solar energy conversion methods [115] is to use solar energy to create different electrical charges. Active power transfer requires an electron charge carrier and a hole to overcome their Coulomb coupling attraction V , which can be denoted by Equation (2);

$$V = \frac{e}{4\pi\varepsilon_{\gamma}\varepsilon_{0}\gamma}. \tag{2}$$

In addition, biological matter has a significantly greater burden of intermolecular charge transmission than inorganic matter. Because charged circuits are concentrated in a small area, there is a greater possibility of recurrence. More importantly, the exciton distribution length and optical absorption depth of organisms are both below 10 nm. The thickness of the active layer ranges from 30 to 100 nm in order to effectively build photographic network systems that are sufficiently thin to efficiently capture an event. Power conversion efficiency improves when more and more features in device processing and design techniques are understood about OPV performance. Single-layer OPVs with Schottky diode structure, pure polymer, and two electrodes have been around from the beginning. The first OPV was proposed in 1986 and was based on a two-layer structure consisting of p-type copper phthalocyanine and n-type perylene diamide. An efficient method for dissociating tightly bound excitons is to use an HJ, which comprises two distinct organic semiconductors with offset power levels (supply and receiver), supply (D) and (A). D^{+}/A charge-transfer circuits are more sensitive to the exciton state of D or A. Electron transfer from composite polymers to C60 was shown to be very fast by Heeger *et al.*, and additional developments in image processing yields allowed the use of polymers treated with an OPV solution. A thin working layer is required to prevent light absorption due to the short dispersion length for exciton ions. One of the most difficult problems in two-layer OPVs was solved in 1992 using a massive heterojunction (BHJ) construction [116]. Dissociation of excitons in the BHJ structure's bicontinuous interpenetrating D–A network provides a huge region of dissociation, reducing the distance between electrodes. It marks a turning point in the development of OPVs since the PCE of OPVs is greatly improved by the production of BHJ. As the Internet of things grows, OPVs are becoming more common in indoor systems. Flexibility, lightweight, and the wide range of colors of OPVs all contribute to this. There are fewer wavelengths and less light output from a typical indoor light source than there are from the standard solar spectrum. There are several advantages of using internal OPVs, including their capacity to fine-tune chain resistance, visual clarity, and active layer thickness. This technology is now capable of producing a PCE of more than 20% in the indoor environment. The OPV cells for indoor use have advanced more in device physics research and critical design approaches than OPV cells for outdoor use. Increased reliance on PV ratings may be attributed in large part to these aspects. Internal OPV cells are the focus of this spotlight on application, which covers their benefits and drawbacks, along with the most current technological developments. An overview of numerous research studies on precise measurement is also provided, along with some suggestions.

7. Solar cell energy

The photovoltaic effect, a chemical and physical phenomenon, is what converts light energy directly into electricity in a solar cell, also known as a photovoltaic cell. Any device that alters its electrical properties such as voltage, current, or resistance when illuminated is considered a photoelectric cell of some kind. Photovoltaic modules, often known as solar panels, are made up of several different types of solar cells [117]. Photovoltaic cells may be powered by either sunlight or artificial light. Near-visible-distance detection of light or another magnetic field and measurement of light intensity are all possible with these image sensors (such as infrared detectors). Photovoltaic cells must meet the following criteria: either light absorption or excitation results in an electron–hole pair. Classification of carriers External power circuit value is derived from the differential output of these carriers. Solar cells are often named after the semiconducting materials they are made up of. They need to have certain features in order to be able to absorb sunlight. In addition, some cells are designed for use on Earth while others are designed to be utilized in orbit. For example, solar cells may be single-junction or multijunction, depending on the spectrum of absorption and separation methods available. First-, second-, and third-generation solar cells are available. Crystalline silicon is a commercially advanced PV technology that blends monocrystalline silicon with polycrystalline silicon in the first generation of cells, also known as conventional, traditional, or wafer-based cells. Second-generation thin-film solar cells, including amorphous silicon, CdTe, and CIGS, which are economically relevant in PV power plants at the scale utilized, constitute integrated PV or an independent energy system. Solar cells in the third generation of growth, known as emerging PV, use microfilm technologies, many of which are still in the research or development stages. A wide variety of organic molecules, primarily organometallic compounds, and inorganic chemicals, are in use. Because these technologies aim to assist in achieving the goal of generating low-cost, high-efficiency solar cells, they have received a lot of interest despite their poor performance and short gravity stability in commercial applications. The "first-generation" panels employ silicon solar cells. Silicon blocks are cut from multicrystalline silicon (multicrystalline silicon cell); monocrystalline silicon cell is manufactured from a single crystal of silicon (monocrystals). Compared to regular silicon solar cells, thin-film solar cells of the "second generation" are less costly to produce since they need fewer materials. Physically, thin-film PV cells use a kind of PV technology as the name indicates. They have a larger surface area but are less efficient than other types. The following is a list of the numerous types of solar cells. Noncrystalline silicon (a-Si) is amorphous silicon. More than a decade old, it is the most sophisticated thin-film technology available today. Some private homes, structures, and distant sites are powered by lithium-ion battery technology. USS Corp is an American solar panel manufacturing firm (Uni-Solar). Solar cell pioneers Sharp and Sanyo are still major participants in the industry today. To create amorphous silicon panels, a tiny coating of silicon material (less than 1 mm thick) is vapor-deposited onto a substrate like glass or metal and allowed to cool. Because it can be deposited on plastic at temperatures as low as 75 °C, amorphous silicon is a good candidate for this purpose. The cell's simplest structure is made up of a single pinned layer sequence. Single-layer cells, on the other hand, lose a significant amount of power when exposed to the sun (between 15% and 35%). Increased electric field strength across the material needs a thin coating to be applied. This, on the other hand, decreases the cell's ability to absorb light and hence its efficiency [118]. As a consequence, tandem or even triple-layer devices have been constructed with p–i–n cells stacked on top of each other. Amorphous silicon solar cells were pioneered by Uni-Solar. In order to capture light from the whole spectrum of the sun, they use a three-layer approach. To put that into perspective, the solar cell is just 1/300th the size of a monocrystalline silicon solar cell. Amorphous solar cells have a yield of about 7%, while crystalline silicon solar cells have a yield of 18%. The Staebler–Wronski effect contributes to the poor efficiency of the amorphous silicon panel, which reduces its energy production from 10% to roughly 7% in the first few hours after it is exposed to sunlight. A smaller number of raw materials are required to manufacture "second-generation" thin-film solar cells, making them less costly to generate than ordinary Si solar cells. Physically, thin-film PV cells use a kind of PV technology as the name indicates. They are only slightly less efficient, although they do need a greater surface area for the same amount of electricity to be generated. The following is a list of the different kinds of solar cells. Amorphous silicon is the name given to the form of noncrystalline silicon (a-Si). Thin-film technology has been on the market for about 15 years now. Distant sites or private homes when not in use are powered by lithium-ion batteries, which are also prevalent in pocket calculators. Amorphous silicon solar cells were initially developed by Sharp, Sanyo, and United System Solar Corp (Uni-Solar). To create amorphous silicon panels, a tiny coating of silicon material (less than 1 mm thick) is vapor-deposited onto a substrate such as glass or metal. Low temperatures, as low as 75 °C, enable amorphous silicon to be deposited on plastic. The p–i–n layers are the essential building blocks of the cell structure. A considerable decline in production is seen when single-layer cells are exposed to the sun (in the range of 15%–35%). The Staebler–Wronski effect is the name given to this process of deterioration in honor of its discoverers, Hans-Martin Staebler. Thinner layers are needed for improved stability in order to produce electric field strength throughout the compound. This, on the other hand, decreases the cell's ability to absorb light and hence its efficiency. The p–i–n cells have been used to create tandem and even triple-layer devices in the industry as a consequence as shown in Figure 8. Amorphous silicon solar cells were pioneered by Uni-Solar. To capture light from the whole solar spectrum, they use a three-layer technique. The solar cell is just 1 μm thick or about 1/300 the size of a monocrystalline solar cell as seen in the Figure 8. Amorphous solar cells have a yield of roughly 5%, while crystalline silicon solar cells have a yield of 18%. The Staebler–Wronski effect, which happens during the first few hours of being exposed to light and lowers an amorphous Si panel's energy yield from 10% to around 7%, is mostly to blame. As a result of their reduced manufacturing costs, amorphous silicon solar cells are very cost-competitive. Solar cells that blend live organisms (photosystem I) with inorganic materials are known as biohybrid solar cells [119]. A perovskite solar cell (PSC) is derived from the ABY_3 crystal structure's perovskite arrangement. With an optical bandgap that ranges from 2.3 eV to 1.6 eV, methylammonium lead trihalide ($CH_3NH_3PbX_3$) is the most extensively used perovskite absorber today. Furthermore, $H_2NCHNH_2PbX_3$ showed promise, with a bandgap between 2.2 eV and 1.5 eV. Small bandgaps are closer to the junction of a single-cell junction than methylammonium lead trihalide; therefore it should be able to function at higher efficiency [120]. Solar cells based on $CH_3NH_3SnI_3$, tin-based perovskite absorbers, have also been shown to have poor energy conversion efficiency. Perovskite solar cells offer a significant advantage over silicon solar cells in terms of processing. In order to produce clean silicon veneers, conventional silicon cells use time-consuming and expensive techniques that involve high temperatures (greater than 1000 °C) and special cleanroom facilities. Wet chemical processing may be used to prepare organic–inorganic perovskite material, which is easier to scale up. For the most part, methylammonium lead trihalides were synthesized employing a variety of soluble and evaporation-based processes. During the processing of the solution, methylammonium iodide and lead halide might be dissolved in a solvent and added to the substrate. Further convective and evaporative self-assembly during spinning produced a thick layer of well-polished perovskite materials because of the material's strong ionic connection. (Organic components also contribute to low crystal temperatures.) Instead of forming a layer, spin-coating uses chemicals like DMSO, GBL, and toluene drops to get the desired result. This may cause problems with the solar cell's performance when simple solutions are treated. Vacancies, platelets, and other faults might occur. It is also possible to manufacture a high-quality crystal film with fine control up to 20 nm in only a few inches of square without the need to employ solvent extraction. Perovskite mixtures are dissolved in NMP and combined with a substrate in this process. Diethyl ether, a second solvent that eliminates NMP specifically, is used to rinse the substrate instead of boiling it. Nothing more than a thin layer of perovskite crystal has been left behind. It is possible to use steam to help in the removal of the halide of lead or lead from the spinal column when it is heated to around 150 °C. Small films with multiple stacks may be used in large regions using this technology, which offers benefits over other technologies [121]. This might have a bearing on the production of multijunction cells. Steam-based methods, on the other hand, create layers that are less pliable. A thin layer of oxide metal veneer may be coated with a layer of a thin film from either technique. Perovskite or dye-sensitive PV cells often use this design. These two processes are both capable of increasing the thickness of the layer. In comparison to silicon solar cells, the process and complexity costs are much cheaper. The solvent residue is minimized when evaporation or evaporation processes are used because they reduce the demand for additional solvents. This approach is quite cost-effective to implement. Materials degrade in natural surroundings, causing efficiency losses in perovskite solar cells, which is a current concern with these devices. A nonphotovoltaic material like cadmium telluride or silicon may be categorized as a form of solar cell, while organic compounds like PCDTBT can be categorized as another. Neither is perfect, but each has its advantages and disadvantages. Currently, industrially efficient inorganic materials convert light to electricity at a rate of more than 20% and enable solar panels to survive for over 25 years. Unfortunately, the necessary components, like as Silicon (Si), may be somewhat expensive. Organic solar cells can be quickly and cheaply manufactured since they are built from low-cost materials that can even be transformed into a liquid solution. On the other hand, living solar cells aspire for more than 10% efficiency even in laboratory sizes. Panel life is estimated in months or weeks rather than years since organisms degrade more slowly under light. People do not want to replace solar panels every six months; therefore, they have not employed living organisms to create them. A solar cell that works using long-lasting inanimate objects with little biological expenses would be remarkable in a perfect society. Perovskite solar cells have made an unexpected comeback in solar energy research in the past few years. An inanimate component is coupled to this living composite, which is composed of components. It is a kind of crystal structure that occurs naturally in several minerals. Compounds have a crystal structure, but they are also complex combinations of a methyl group and organic ammonia with inert lead iodide, forming a mixed compound.

There is a lot of enthusiasm about these resources because of the amount of growth they have experienced. Research on a new product used to take 10–20 years to gain even 10% efficiency. Now, it just takes a few months. Although perovskite solar cells were just released in 2012, about 19% of functional changes have already been avoided by these devices. The field of solar research has never witnessed such rapid advancements. Additionally, perovskites, as a hybrid, may employ solar energy to create a water solution. By spraying liquid perovskite over a substrate, Professor David Lidzey’s team at the University of Sheffield took advantage of this phenomenon. Higher density and reduced prices are possible because of this [122].

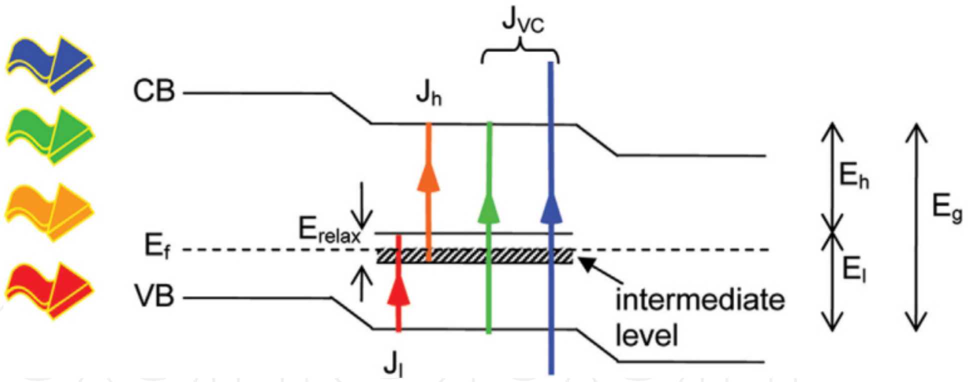

Figure 8. Band diagram of a solar cell with an intermediate band [122].

Questions remain concerning the environmental effect of lead content (although efforts to eliminate the need for lead are ongoing) and the ease with which manufacturing may be raised to the quantity necessary for a meaningful sale. A few droplets of water may completely damage their long-term stability, much like living solar cells. As far as we know, there is no guarantee that perovskite solar panel modules that can survive outdoors for many decades will ever be developed. Although perovskite solar cells have a great level of certainty, if the potential of material objects can be achieved, solar energy will be drastically modified. Solving a long-standing problem in solar cell production, intermediate metallic band materials have been found. Boosting solar cell efficiency beyond Shockley and Queisser's [123] efficiency range, this content uses photon energy below the bandgap. It is possible to employ lower-power light when there is a medium power difference, and two photons can transfer the carrier from one band to the other. Unfortunately, these standards operate as strong integration sites, leading to considerable deterioration of the material in question. This problem may be alleviated to some extent by inserting the thin metal band into a huge semiconductor gap. This band prevents nonradioactive reunion. Since the metal band has a low concentration of both holes and electrons, the neutral charge is always generated.

7.1. Long-term stability of perovskite solar cells

Traditional thin-film solar cells cannot match the efficiency of PSCs when it comes to converting sunlight into power. Making the perovskite as stable as other compounds is the next apparent problem. Research on the stability of PSCs is difficult to understand due to the lack of standardized aging test conditions. To make matters worse, stability data obtained from the J–V curve tends to overstate performance on older hardware. Therefore, we only publish outputs that have been confirmed across many groups rather than inside a single research under particular testing conditions. The PSC stability is affected by a wide range of possible degradation impacts. When it comes to performance loss, humidity is by far the most aggressive culprit. Perovskite and compounds in the device may degrade as a result of external factors [124]. Encapsulation methods differ in their ability to effectively isolate the device from these outside sources of deterioration. Even under inert conditions, inherent instability is a considerably more serious threat. These may have an impact on the device's perovskite and other components. The reduced electronic contact between perovskite and metal electrodes caused by the crystallization of small molecule hormone-sensitive lipase (HSL) at relatively high temperatures reduces device performance. When it comes to lab-scale PSC production, gold has been a popular top metal contact. Gold migration inside small molecule HSLs produces dramatic performance losses when evaluated at a tolerable temperature. As a consequence, the drop in performance is mostly due to this impact. For the investigation of small molecule HSLs, gold migration has to be prevented. Although carbon-based HSLs tend to be less efficient than organic HSLs, they are a more reliable option. To our surprise, polymeric HSLs, chromium interlayers, and alumina nanoparticle buffer layers all were effective in preventing gold from migrating through their surfaces. There is less thermal stability in small molecules than polymeric HSLs, which are stable throughout the solar cell's temperature range of operation. Metal oxides used as ESLs are affected by the degradation process that is initiated by UV light. Increasing the PSC's UV stability may be accomplished by the application of chemical doping to either stabilize metal oxides or lower the metal oxide content [125]. A stable perovskite layer is essential for a commercially successful PSC technology since it is the device's core. Perovskite preparation and device operation introduce ionic defects, as has been well documented and handled earlier. Due to the fact that these defects form acceptor and donor electronic states close to or within conduction and valence bands, they do not seem to be extremely detrimental to the majority of the perovskite layer. A fault may spread from the bulk of perovskites to its edges at a selective contact interface with ionic imperfections. Space charge layers may develop up here, reducing the efficiency of charge extraction. Space charge may be greatly reactivated if selective contact is made at the interface. The interface between perovskite and selective contact seems to have a role in device stability, while its possible inherent instability is still being researched. It is possible to improve device stability by reducing the number of defects through the use of various perovskite chemical doping, surface passivation, or composition surface passivation methods [126].

7.2. Preparation techniques

The two most frequent thin-film fabrication processes are complementary in terms of material selection. While evaporation requires thermal stability, solution processing necessitates solubility and vice versa. Although molecules may be more thermally stable, this does not mean they are more soluble than polymers, which often acquire solubility via the solubilization of their side chains. It is impossible to evaporate polymers because they degrade at high temperatures and have a high molecular mass. As a consequence, evaporation is the optimal choice for small molecules, while semiconducting polymers are often developed from a solution. Solubilizing groups (e.g., PCBM) may be used to make less soluble chemicals, such as C60, more soluble, and short polymers and oligomers can be evaporated [127].

Evaporation: Using a vacuum of 105 mbar, the mean free path of the evaporated molecule is greater than the distance between the sample and the evaporation source, making it possible to build a film. Other contaminants like oxygen and water may also be removed by utilizing an ultrahigh vacuum (109 mbar) or an inert atmosphere to evaporate them. Co-evaporation methods may be utilized to build an interpenetrating donor–acceptor network or achieve molecular doping. All wet processes use a solution of organic molecules in a suitable solvent, such as water or any other nonpolar or polar organic solvent. The soluble monomer is processed for film formation during, e.g., electrochemical polymerization, or immediately after, e.g., heat treatment, UV curing, and so on, in combination with polymerization reaction (precursor route). This has the advantage of making the polymers insoluble, enabling another layer to be deposited on top of them from the solution. Polymer, polymer/polymer, and polymer/molecule mixtures may be treated directly from solution in a variety of ways: (a) spin-coating, (b) doctor-blading, (c) screen printing, and (d) inkjet printing. In the MDMO-PPV:PCBM mix, for example, screen printing was used [128]. Because current printing processes are being used, solar cell manufacture can be scaled up quickly while using less energy, which is crucial for amortization (energy delivered by the solar cell during its lifetime as compared to the energy needed to produce the solar cell itself).

8. Optoelectronics

Organic (opto-) electronics have received a lot of attention because of their use in thin-film transistors, light-emitting diodes, solar cells, sensors, photorefractive devices, and other applications. This technology's promise includes affordable materials and room-temperature application from a solution across a large surface. In this article, the present level of knowledge regarding the physical principles that define the most efficient (opto-) electrical structures in living organisms is discussed. An optoelectronic system based on network corporate image production is analyzed, with particular attention paid to image processing methods and electrical equipment. Additionally, this highlights its capacity to do numerous measurement tests on these systems as well as summarize and outline the most current advances in the ever-evolving field [129]. Organic solar cells, photodetectors, photorefractive

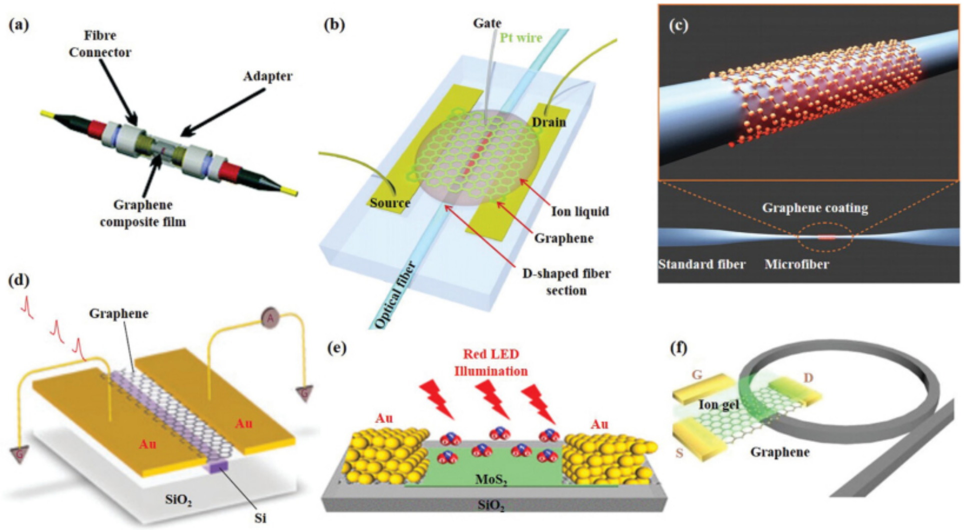

Figure 9. Common 2D-material-based optoelectronic structure uses [131].

devices, and the properties of materials consisting of small molecules and composite polymers are discussed. When a semiconductor device is used to convert light into electrical energy or the other way around is known as optoelectronics. These devices are built of solid crystalline materials, which are lighter in weight than metal but heavier than insulators. Light-based electronic devices are known as optoelectronic devices. Telecommunications, military services, automated access control systems, and medical equipment are examples of applications where this type of gadget is used. Lasers, optical fibers, LED streetlights, photodiodes, and solar cells are examples of optoelectronic devices [130]. There are several applications for LEDs in the home and at the workplace. LEDs may be used as indicator lights in computers, medical equipment, clocks, metal panels, switches, and fiber-optic communication systems. They are also employed in a range of electrical engineering and electronic applications including propeller displays using virtual LED based AEL. LED street lights with auto-intensity control and display of colored phone numbers on seven-segment screens mostly use solar-powered LED lights.

8.1. Composite structures and applications

Fiber optics and on-chip 2D-material-based optoelectronic devices are divided into two structural categories based on material attributes and optical structure.

Figure 9a shows a 2D material deposited on the fiber end-facet; Figure 9b shows a D-shaped fiber with a 2D material placed on the top surface; Figure 9c shows a 2D-material-wrapped microfiber as a typical optical-fiber/2D-material composite construction (Figure 9c). Ultrafast lasers and sensors may profit greatly from the use of 2D materials and optical fiber systems. With regard to ultrafast lasers that utilize 2D materials, a saturated absorber is frequently created by depositing 2D materials on the ends of an optical fiber; their saturation absorption impact is used to produce the saturated absorber, such as just one layer of graphene that absorbs 2.3% of incoming light from the vertical direction [131]. For the 2D materials attached to the microfiber and deposited on the D-shaped fiber, the light–matter communication duration and separation are longer than the time for deposit.

Due to the large insertion loss and lengthy light–matter interaction distance and duration, these two structures are often used in sensor design and are seldom used in lasers since they result in a considerable increase in sensor sensitivity. External factors may be used to alter the conductivity of a 2D material and hence alter the optical field of an optical cable.

For 2D materials and transfer processes, the on-chip platform has more requirements than the optical fiber platform, but it is more integrated. 2D-material-based chip platforms, such as waveguides (Figure 9d), SiO_2 substrates (Figure 9e), and microrings (Figure 9f), have been extensively employed in optical communication systems (including detectors, modulators, and lasers) and fundamental research (including nonlinear optics, optical frequency combs, and plasmon). The bulk of these applications depend on on-chip platform bipolar junction transistors and field-effect transistors (FETs) made of two-dimensional materials (FETs). It has tremendous potential in domains such as functional and information science applied to optoelectronic devices.

8.2. Carbon nanotubes for electronic and optoelectronic applications

With its quasi-one-dimensional structure and a vast variety of electrical characteristics based on chirality, CNTs have a lot of potential as electronic materials. While metallic CNT thin films might be used to transmit electricity through a transparent layer, semiconducting CNT channels have the potential to be utilized in FETs. In a CNT FET, two electrodes are connected to the CNT, and electricity flows between them (source and drain) [132]. The CNT carrier density is modulated by the third electrically isolated electrode, allowing it to be switched (gate). To begin, we will go over the fundamentals of CNT charge transfer and why these materials are so useful in electrical engineering. Low switching energies, excellent gate coupling, and minimum parasitic capacitance for low-power, high-speed electronics are all made possible by the small capacitance of CNTs (0.05 aF/nm). CNTs also minimize carrier dispersion, making them more mobile. This is due to CNTs' atomically flat surface and lack of protruding bonds. Traditional semiconductor technologies have a high level of surface state and interface roughness, which may be reduced by the use of CNTs. Lastly, because of their one-dimensional structure, CNTs do not suffer from small-angle carrier scattering. Acute defects and high-energy optical phonons can only provide the momentum transfer required for carrier backscattering, and so it is reduced at low-field conditions [133]. Long-range Coulomb scattering is also wasteful; therefore the elastic mean free path in CNTs may be as small as a few microns in diameter. Acoustic phonons and the RBM phonons, on the other hand, may generate a significant amount of inelastic scattering. This inverse relationship between temperature and carrier mobility is seen in one-dimensional CNTs, as opposed to the $1/T_5$ behavior observed in three-dimensional metals. In contrast to other high-mobility semiconductors like InSb, which can have extremely high low-temperature movement but significantly lower room temperature movement, CNTs may exhibit very high low-field movement at room temperature. Consequently, field-effect mobilities over 100,000 cm^2/Vs and current densities up to 108 A/cm^2 have been observed in CNTs at ambient temperature without electromigration [134]. Metallic CNTs experience current saturation whereas semiconductors experience velocity saturation when subjected to high bias. Impact excitation may be induced at even higher energies by strong electron–electron interactions. Because CNTs are one-dimensional, they cannot be used in nanoelectronics. When a one-dimensional CNT comes into contact with a three-dimensional metal electrode, the contact resistance drops to its fundamentally lowest value (6.45 Ω) [135]. Most metals and CNTs have Schottky connections that enhance contact resistance, unlike the ohmic contact in Si FETs. Because CNT FETs are inherently ambipolar, the difference between the metal work function and the Fermi level of the CNTs may be controlled to permit both n-type (electron-conducting) and p-type (hole conducting) FETs [136]. Unless the electrode or doping work function is deliberately altered, CNT FETs in ambient conditions tend to operate in the p-type mode due to air adsorbates such as oxygen. In addition, because of their inherent band structure, CNTs have a quantum capacitance of 10–16 F/m, which depends on carrier density. When used with ultrathin high gate dielectrics, a CNT FET's performance may be constrained by quantum capacitance instead of geometric capacitance. CNTs are suitable for designing novel optoelectronic devices because of their unique optical properties. There exist both free electron–hole pair excitations and securely bound electron–hole pair states in semiconducting CNTs, which are straight bandgap materials. Optical emission and absorption occur in large quantities due to van Hove singularities in state densities that are caused by the one-dimensional structure of CNTs. Compared to typical bulk semiconductors like GaAs, the exciton binding energy in CNTs is several hundred times higher (10 meV). Due to the huge binding energy of 1D excitons (up to 100 ns) and fluorescent lifetime (up to 100 ps), exciton dynamics may be easily analyzed at room temperature [137] (as opposed to the III–V semiconductor coupled quantum-well heterostructure, which requires extensive manufacture). Electroluminescence and photoluminescence may be generated in CNTs by the recombination of excitons, which occurs both optically and electrically.

Electroluminescence in CNTs has been observed in ambipolar and unipolar FETs using impact excitation at room temperature [138].

9. Current and future photocatalytic applications

9.1. Hybrid/composite photocatalysts

Photocatalytic reactors are of use in catastrophes and floods as they can be utilized for treating flood water to aid flood-affected persons as well as for treating wastewater. They may be employed in the future to prevent the dengue virus. More and more applications for nano-TiO_2 photocatalysis are being explored, including graphene-based composite catalysis, nano-TiO_2 photocatalysis in combination with membrane separation technology, nano-TiO_2 doping, and self-cleaning nano-TiO_2. Nano-TiO_2 photocatalysis enhancement methods. Graphene-based photocatalysts, hybrid/composite photocatalysts, catalyst doping, optimal conditions, and a suitable substrate for immobilization may all boost photocatalytic activity when used in conjunction with an efficient light distribution system [139].

Composite photocatalysts made of graphene: In recent years, carbon-based materials have emerged as a new form of tailored photocatalysts. Many researchers are interested in graphene–nano-TiO_2 photocatalyst coupling because of the large specific surface area and strong electron mobility it provides. In graphene-based TiO_2 photocatalysis, electrons liberated from TiO_2 are expected to move to graphene and therefore avoid recombination [140]. Extending the lifespan of photoexpelled electron–hole pairs is another benefit of TiO_2 interfacial charge transfer. Compared to the typical H electrode (NHE), 2.81 V and 0.39 V are the observed VB and CB energy levels, respectively, in TiO_2. The graphene's Fermi level (0.08 V vs NHE) permits photogenerated electrons to flow from TiO_2 to the graphene. Thus, graphene may serve as an electron collector. Increased photocatalytic effectiveness of graphene-based photocatalysts is predicted due to graphene's improved unique charge-transfer capabilities [141]. According to a study of the literature on immobilized graphene-based TiO_2, mechanical mixing or chemical bonding may be used to integrate graphene with nano-TiO_2. Chemically bonded composites are able to produce a tight interface between TiO_2 nanoparticles and graphene sheets [142], but mechanically mixed composites cannot. In order to reduce the risk of electron–hole recombination, strong contact facilitates electron transport. Composites that are chemically linked have higher photocatalytic activity. Excellent spatial conditions for the charge transfer from nano-TiO_2 to graphene are credited for enhanced photocatalytic activity. As a result, graphene/TiO_2 composite catalysts have been more widely used in photodegradation processes [143]. As the bandgap of the graphene/TiO_2 hybrid decreases, it becomes easier to use visible light. The graphene/TiO_2 composite's bandgap was found to be reduced from 3.18 eV (in the instance of P25) to 2.95 eV. Small bandgaps in TiO_2 were caused by the chemical interactions between TiO_2 and carbon as well as the movement of the VB edge up. Bandgap shortening techniques often treat intermediate energy levels as a sequential process with the lowest and highest energy states being accessible. Because the TiO_2 composite catalyst uses graphene oxide as the sensitizer, solar energy is a cost-effective method. There is yet no information on the graphene/TiO_2 composite's ability to absorb visible light. Graphene structural faults must be eliminated despite recent advances if charge-transfer control is to be improved [144].

9.2. A method of preventing dengue utilizing a photocatalytic reactor

As a result of the lack of scientific knowledge of human–insect interactions, dengue fever is a viral illness with an alarmingly high incidence. Nearly fifty million individuals are infected with dengue fever each year [145], making it the most frequent arthropod-borne illness in the world. In recent years, dengue fever has become a major pandemic in Pakistan. In 2011, it claimed the lives of tens of thousands of people and wreaked havoc in three Pakistani provinces. It is merely a short-term fix to spray pesticides on Aedes aegypti (the dengue virus's primary vector). We were able to effectively disinfect the coliphage MS_2, plague virus, and Chinese hamster utilizing nano-TiO_2 photocatalysis. It is possible that the hydroxyl radical generated by photocatalytic activity would interfere with the hatching of Aedes aegypti eggs and damage organic matter, including the larvae's food supply and potentially the larvae themselves. Mathematical modeling, statistical analysis, and site selection were used to determine the placement of the prototype photocatalytic reactor for dengue control. Cancer cells are killed by the TiO_2 particle's photocatalytic activity. Biophotoconductivity and maximal hydroxyl radical production may be found in thin films of nanostructured TiO_2/Ag, TiO_2, and TiO_2/Ag/Ni. Oxyl radicals were generated using a floating autoclaved brick coated with an iron-oxide-based catalyst [146]. Both dengue virus larvae that had hatched and those that had previously hatched were killed by the photocatalytic activity. After treating outdoor air and purifying interior air with UV radiation, the reactor would irradiate open areas with UV radiation in an effort to weaken the dengue virus and eliminate it. UV light may also be used to clean the air in air conditioners. Freshwater ponds and lakes might be eliminated as breeding grounds by using reactors with a sustainable design. On the other hand, commercially available sprays comprising TiO_2 and ZnO nanoparticles would be developed.

10. *Future challenges and Goals*

10.1. Perspective and challenges

A broad variety of insecticides and pesticides may be destroyed effectively using semiconductor photocatalytic technology, which makes use of UV radiation or sunlight. Since organic matter is made up of minerals, this is especially relevant. Photocatalytic H_2O purification technology will soon be a feasible option when paired with the circular process. Water that has been polluted by pesticides, weedkillers, or disinfectants may be disinfected using this photocatalytic approach. There are a few significant technological problems that need to be researched further in water treatment technology with heterogeneous photocatalytic activity [147, 148]. Photocatalytic procedures should be analyzed to determine if they are pretreatment phases or standalone programs.

A photocatalytic technique may be employed as a prior treatment step to encourage environmental degradation of refractory contamination before natural water purification since nonbiodegradable water-soluble contaminants have a nonselective reaction as shown in Figure 10. As a consequence, the photocatalyst dosage may be greatly lowered during the reaction. The photocatalytic technique is effective when used on its own [149, 150]. To properly activate germs and minerals, the treatment strategy and the duration may need to be longer.

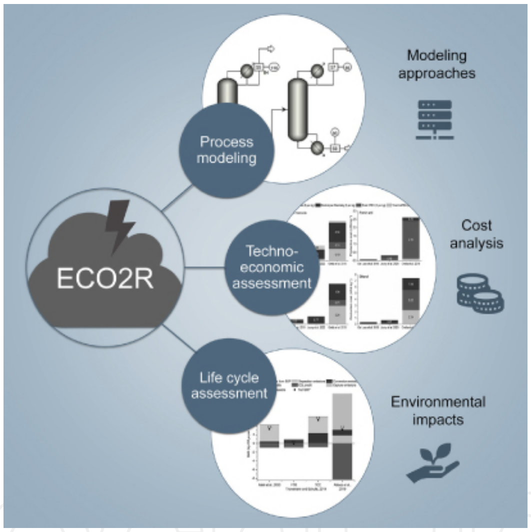

Figure 10. Life cycle impact evaluation findings for the alternatives under consideration [151].

Sluggish kinetics, poor picture quality, and the need for continuous (noninterrupted) illumination are all problems when trying to remove organic carbon or kill microbes. The extra reaction volume expenses may be offset by the site-location requirements of the standalone system. The photocatalytic fluid has various technological hurdles to overcome. These include catalyst development, reactor design, and process optimization, which must be overcome quickly in order to boost the technique's applicability. A novel integrated system for improved photomineralization or photodisinfection kinetics is; (iv) an effective design of the photocatalytic reactor system or a parabolic solar collector for the high sola; and (v) a combination of catalyst immobilization technique to deliver less costly so liquid separation. Now only 5% of the solar spectrum can be used due to a bandgap in TiO_2 photocatalysts [152]. A UV procedure is used because bacteria need steady light to thrive; this means that sunlight is used to power this process. Photocatalytic technology in the water treatment industry is motivated by the existing solar collecting technology's poor efficiency (0.04% of the initial photons captured by solar panels) [153]. An additional evaluation of test equipment with a new reactor is necessary to confirm that the well-established photocatalytic water technology provides highly productive technical and economic data for any LCA. A photocatalytic treatment facility for ground-based and sun-driven demands can be built quickly with the speedy testing of various alternatives and the creation of experimental plants.

Currently, the main issue is efficiency and implementation in commercial markets. Most of these challenges can be solved by enhancing efficiency and production rates. Solar cell plates did not produce sufficient energy to meet demands. But recently, smart solar cells have been manufactured to enhance efficiency and for commercial purposes.

10.2. Future outlook and Goals

The past decade has seen a boom in research on graphene and other two-dimensional compounds including transition metal dichalcogenides (TMDs), MXenes, black phosphorous (BP), and others. A wide range of two-dimensional material based optoelectronic devices (ultrafast lasers, frequency converter devices—such as photodetectors and modulators—sensors, and plasmonic generators) have been developed so far.

There is a lot of potential in 2D materials for optoelectronic devices, as shown by all of these contributions. In the past, however, the bulk of studies focused on the qualities of materials and hypothetical gadgets. We still face considerable difficulties in the actual execution, which might potentially offer great scope. It is our hope that this report will throw some light on future research by providing a subjective evaluation of current trends and major directions in the field. Optoelectronic devices [154, 155] employ materials other than glass. Research on TMDs and BP has lagged behind that of graphene because of the latter's dominant band structure and spectral response characteristics [156–159]. Van der Waals heterostructure based functional optoelectronic devices are created to address specific application demands, such as ultrafast lasers, high-speed modulators, ultrasensitive sensors, ultrahigh responsivity photodetectors [160], and ultralow gaming plasmonics. New metamaterials, such as perovskite and topological insulators, are being investigated for use in optoelectronics. For example, functional inks and 2D-material printing are being explored to provide new 2D-material preparation procedures. Phonon lasers and exceptional points (EPs) for 2D-material-based optoelectronic systems are under investigation [161].

A highly integrated, multipurpose optical device may be easily and economically implemented into photonic integrated circuits owing to recent improvements in the fabrication process of 2D materials. To create 2D materials, modification is equally crucial. There are a number of techniques that may be used to minimize the drawbacks of materials and maximize their advantages. There are a broad variety of uses for 2D-material optoelectronic devices. An overview of this article is presented in Figure 11. Many studies have yet to move beyond the theoretical stage. In terms of actual applications, there are still many challenges and possibilities to be overcome.

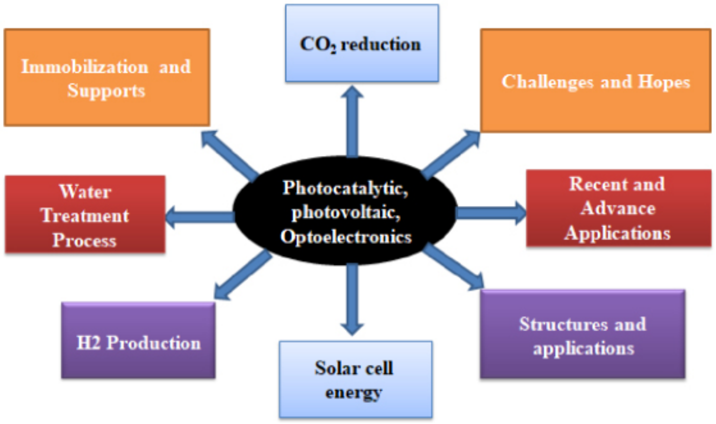

Figure 11. An overview of this review article.

After only a decade of development, perovskite solar power has demonstrated its potential for commercialization. Exciting properties like high specific power, cheap production costs, and improved low-light performance have provided significant value in multiple uses, distinguishing it from comparable technologies. In the beginning, we look at the most prevalent deposition processes used in labs and enterprises to coat perovskites. Subsequently, the key parameters to consider when constructing a module are discussed. For instance, to minimize moisture and O_2 damage, the produced modules must be packaged robustly. Furthermore, we address the perovskite's technological contact with rapidly emerging areas as well as the prospects that exist [162]. Finally, we assess the perovskite [163] module's ecological impact through life cycle evaluation and proper recycling procedures to ensure longevity as well as improve energy turnaround time.

11. Conclusion

Development in perovskites prepared from $KGaO_3$ and $RbCa_2Mg_3O_{10}$ as well as progress in the use of oxide-based photocatalysts in UV following the visible range of the solar spectrum has been achieved, which have been highlighted in this article. Alkali formation, halides, and oxides and methods for using them as effective solar energy converters and natural corrective materials as well as giving insight and advice for future research were our primary goals. More research is required to produce alkali-metal-based perovskites for practical use in solar photocatalytic energy conversion and environmental improvements to ensure a sustainable and secure future. According to the review of processes for synthesizing perovskites, several reactions have an impact on the morphology and structure of oxide and halide perovskites. It indicates that a combination of high temperatures may be achieved using reverse micellar and hydrothermal synthetic techniques. As a result of these low-temperature techniques, photocatalytically active coatings may be produced. Photocatalysis shows another way to overcome energy and other environmental concerns as fundamental research advances in this field. There are several difficulties for CO_2, NiO_2, and TiO_2 photocatalysts to overcome, including poor photocatalytic activity due to the increasing need for energy and industrial growth. A photocatalyst must be able to absorb a significant amount of light in order to be effective. Absorption of light is the first stage of photocatalysis, and the quantity of energy absorbed directly influences how many electrons or holes are generated, affecting photoefficiency. To use catalysts in the visible spectrum, a variety of techniques, including doping, HJ creation, Z-scheme idea, and primary shell nanocomposites, are applied. Even though photocatalytic effectiveness depends on light absorption, it has nothing to do with the overall function of photocatalysts. It is thus imperative that photocatalysis be improved in order to maximize light absorption. By increase case segregation photocatalysis, reunification sites such as holes and deformities should be decreased or removed. It is true that a few of the strategies discussed in this review, such as the development of HJs (e.g., C_3N_4/nanostructure) and metal–semiconductor composites (e.g., CdS/nanostructure), can improve charge separation and provide an energy-enhanced built-in electricity field, but the driving force/electric field is relatively low. As a consequence, the charging efficiency of all devices will be improved by the use of manufacturing materials with greater internal electric fields. Alkaline perovskite photocatalysts have been studied extensively, but there is still more work to be done in this area. To enhance weak photocatalytic activity in the future, work on performance methodologies, sophisticated character classification procedures, and theoretical calculations is required. There are also environmental benefits, such as a reduction in greenhouse gas emissions and more cost-efficient goods, to producing active metal-oxide crystals utilizing the growth technique.

Conflict of interest

The author declares no conflict of interest.

References

1 Maeda K. Photocatalytic water splitting using semiconductor particles: history and recent developments. *J Photochem Photobiol C: Photochem Rev*. 2011;**12**(4):237–268.

2 Qu Y, Duan X. Progress, challenge and perspective of heterogeneous photocatalysts. *Chem Soc Rev*. 2013;**42**(7):2568–2580.

3 Cook TR, Dogutan DK, Reece SY, Surendranath Y, Teets TS, Nocera DG. Solar energy supply and storage for the legacy and nonlegacy worlds. *Chem Rev*. 2010;**110**(11):6474–6502.

4 Shahzad MK, Hussain S, Riaz M, Sattar H, Ashraf GA, Azeem W, et al. Investigation of ultra wide bandgap Flouro-perovskite materials $RBeF_3$ (RK and Li) for smart window applications: a DFT study. *Heliyon*. 2024;**10**(7):e29143.

5 Tekalgne MA, Kim SY. Research progress and perspectives on photocatalysts based on the lead-free double halide perovskite. *EES Catal*. 2024;**2**: 94–108.

6 Shahzad MK, Hussain S, Farooq MU, Abdullah A, Ashraf GA, Riaz M, et al. First principle investigation of tungsten based cubic oxide perovskite materials for superconducting applications: a DFT study. *J Phys Chem Solids*. 2024;**186**: 111813.

7 Masri M, Hezam A, Alkanad K, Prashantha K, Manjunath S, Masri F, et al. Metal halide perovskite-based photocatalysts for organic pollutants degradation: advances, challenges, and future directions. *Colloids Surf A: Physicochem Eng Asp*. 2024;**687**: 133387.

8 Dhariwal S, Mittal M. Wastewater treatment with perovskite-based photocatalysts: environmental sustainability from a green perspective. *Mater Today: Proc*. 2023; doi: 10.1016/j.matpr.2023.03.048.

9 Hussain S, Rehman JU. First-principles calculation to investigate structural, electronic, optical, and thermodynamics properties of perovskite KXO_3 (K = Ta and Zn) alloys for photovoltaic and smart window applications. *Phys B: Condens Matter*. 2024;**687**: 416116.

10 Hantusch M, Bessergenev V, Mateus MC, Knupfer M, Burkel E. Electronic properties of photocatalytic improved Degussa P25 titanium dioxide powder. *Catal Today*. 2018;**307**: 111–118.

11 Kadkhodayan H, Alizadeh T. Manufacturing visible-light-driven heterojunction photocatalyst based on MOFs/$Bi_2WZnTiO_9$ triple perovskite/carbonous materials for efficient removal of poisons, antibiotics, and inorganic pollutants. *J Phys Chem Solids*. 2023;**183**: 111620.

12 Stranks SD, Eperon GE, Grancini G, Menelaou C, Alcocer MJ, Leijtens T, et al. Electron–hole diffusion lengths exceeding 1 micrometer in an organometal trihalide perovskite absorber. *Science*. 2013;**342**(6156):341–344.

13 Singh T, Kulkarni A, Ikegami M, Miyasaka T, Miyasaka T. Effect of electron transporting layer on bismuth-based lead-free perovskite $(CH_3NH_3)_3Bi_2I_9$ for photovoltaic applications. *ACS Appl Mater Interfaces*. 2016;**8**(23):14542–14547.

14 Nagaveni K, Sivalingam G, Hegde MS, Madras G. Solar photocatalytic degradation of dyes: high activity of combustion synthesized nano TiO_2. *Appl Catal B: Environ*. 2004;**48**(2):83–93.

15 Aldeen ES, Jalil AA, Mim RS, Hatta AH, Hazril NIH, Chowdhury A, et al. Environmental remediation of hazardous pollutants using MXene-perovskite-based photocatalysts: a review. *Environ Res*. 2023;**234**: 116576.

16 Asiri AM, Shahzad MK, Hussain S, Zhu K, Khan SB, Alamry KA, et al. Analysis of $XGaO_3$ (X = Ba and Cs) cubic based perovskite materials for photocatalytic water splitting applications: a DFT study. *Heliyon*. 2023;**9**(3):e14112.

17 Raeisipour J, Salari D, Niaei A, Hosseini SA, Maleki A. $Co_{1-n}SrTiO_3$ (n = 0, 0.05, 0.1) nano perovskites: novel photocatalysts synthesized by sol-gel and cold-evaporated sol-gel methods for CO remediation from polluted air. *Ceram Int*. 2024;**50**(11, Part A):18125–18137.

18 Zhang H, Chen G, Li Y, Teng Y. Electronic structure and photocatalytic properties of copper-doped $CaTiO_3$. *Int J Hydrogen Energy*. 2010;**35**(7):2713–2716.

19 Melo MA, Carminati SA, Bettini J, Nogueira AF. Pillaring and NiO_x co-catalyst loading as alternatives for the photoactivity enhancement of $K_2Ti_4O_9$ towards water splitting. *Sustain Energy Fuels*. 2018;**2**(5):958–967.

20 Hussain S, Rehman JU. First-principles calculations to investigate structural, electronics, mechanical, and optical properties of $KGaO_3$ cubic perovskite for photocatalytic water-splitting application. *Optik*. 2023;**291**: 171326.

21 da Silva Alves DC, de Farias BS, Breslin C, de Almeida Pinto LA, Junior TRSAC. Carbon nanotube-based materials for environmental remediation processes. In: *Advanced materials for sustainable environmental remediation*. Amsterdam: Elsevier; 2022. p. 475–513.

22 Niharika MP, Garlapallya R, Ruthvik K, Velaga M, Rao BM. Hydrogen production on $g\text{-}C_3N_4$ nanoflakes via photoelectrochemical water splitting. *Mater Today: Proc*. 2023; doi: 10.1016/j.matpr.2023.06.188.

23 Esfe MH, Alidoust S, Hatami H, Toghraie D. Rheological behavior of 10W40 base oil containing different combinations of MWCNT-Al_2O_3 nanoparticles and determination of the target nano-lubricant for industrial applications. *Micro Nano Syst Lett*. 2023;**11**(1):14.

24 Behera SA, Amanat A, Achary PGR. Photocatalytic degradation of ciprofloxacin drug utilizing novel PVDF/polyaniline/lanthanum strontium manganate@ Ag composites. *J Met Mater Miner*. 2024;**34**(1):1896.

25 Ali SA, Ahmad T. Treasure trove for efficient hydrogen evolution through water splitting using diverse perovskite photocatalysts. *Mater Today Chem*. 2023;**29**: 101387.

26 Mera A, Rehman MA, Ur Rehman Z, Farrukh U, Usman M, Rehman A. Computational exploration of oxide-based double perovskites Sr_2MgWO_6 and Ba_2BiVO_6 for photocatalysts for sustainable degradation processes. *Inorg Chem Commun*. 2024;**162**(1–3):112259.

27 Shahzad MK, Mujtaba ST, Hussain S, Rehman JU, Farooq MU, Khan MA, et al. Zirconium-based cubic-perovskite materials for photocatalytic solar cell applications: a DFT study. *RSC Adv*. 2022;**12**(42):27517–27524.

28 Shen L, Kang H, Deng L, Chen Z, Yang MQ. Solvent-free oxidation of benzylic C (sp^3)–H bond over $MA_3Bi_2Br_9$ perovskite photocatalyst by efficient singlet oxygen generation. *J Catal*. 2024;**434**: 115499.

29 Byun MY, Kim YE, Baek JH, Jae J, Lee MS. Effect of surface properties of TiO_2 on the performance of Pt/TiO_2 catalysts for furfural hydrogenation. *RSC Adv*. 2022;**12**(2):860–868.

30 Pal B, Mathuri A, Manna A, Mal P. $CsPbBr_3$ perovskite photocatalyst in chemodivergent functionalization of N-Methylalkanamides using CBr_4. *Org Lett*. 2023;**25**(22):4075–4079.

31 Hussain S, Rehman JU, Hussain A, Tahir MB, Iqbal F. Study of double perovskite materials $RbX_2Y_3O_{10}$ (XMg, Ca, YTi, Zr) for photocatalytic applications: a DFT insights. *Int J Hydrogen Energy*. 2024;**62**: 739–748.

32 Lykos C, Tsalpatouros K, Fragkos G, Konstantinou I. Synthesis, characterization, and application of Cu-substituted $LaNiO_3$ perovskites as photocatalysts and/or catalysts for persulfate activation towards pollutant removal. *Chemosphere*. 2024;**352**: 141477.

33 Rahimi N, Pax RA, Gray EM. Review of functional titanium oxides. I: TiO_2 and its modifications. *Prog Solid State Chem*. 2016;**44**(3):86–105.

34 Stolarczyk JK, Bhattacharyya S, Polavarapu L, Feldmann J. Challenges and prospects in solar water splitting and CO_2 reduction with inorganic and hybrid nanostructures. *ACS Catal*. 2018;**8**(4):3602–3635.

35 Yang K, Yang Z, Zhang C, Gu Y, Wei J, Li Z, et al. Recent advances in CdS-based photocatalysts for CO_2 photocatalytic conversion. *Chem Eng J*. 2021;**418**: 129344.

36 Kumagai H, Tamaki Y, Ishitani O. Photocatalytic systems for CO_2 reduction: metal-complex photocatalysts and their hybrids with photofunctional solid materials. *Acc Chem Res*. 2022;**55**(7):978–990.

37 Álvarez A, Bansode A, Urakawa A, Bavykina AV, Wezendonk TA, Makkee M, et al. Challenges in the greener production of formates/formic acid, methanol, and DME by heterogeneously catalyzed CO_2 hydrogenation processes. *Chem Rev*. 2017;**117**(14):9804–9838.

38 Sun Z, Wang H, Wu Z and Wang L. g-C_3N_4 based composite photocatalysts for photocatalytic CO_2 reduction. *Catal. Today*. 2018;**300** 160–172. Available from: https://www.sciencedirect.com/science/article/abs/pii/S0920586117303425?via%3Dihub.

39 Ma Y, Wang S, Duan X. Recent advances in direct gas–solid-phase photocatalytic conversion of CO_2 for porous photocatalysts under different CO_2 atmospheres. *Chem Eng J*. 2023;**455**: 140654.

40 Koppenol WH, Rush JD. Reduction potential of the carbon dioxide/carbon dioxide radical anion: a comparison with other C1 radicals. *J Phys Chem*. 1987;**91**(16):4429–4430.

41 Hou J, Cao S, Wu Y, Gao Z, Liang F, Sun Y, et al. Inorganic colloidal perovskite quantum dots for robust solar CO_2 reduction. *Chemistry–A Eur J*. 2017;**23**(40):9481–9485.

42 Liu Z, Hou W, Guo H, Wang Z, Wang L, Wu M. Functional group modulation in carbon quantum dots for accelerating photocatalytic CO_2 reduction. *ACS Appl Mater Interfaces*. 2023;**15**(28):33868–33877.

43 Dresselhaus MS, Thomas IL. Alternative energy technologies. *Nature*. 2001;**414**(6861):332–337.

44 Yang J, Hou Y, Sun J, Liang T, Zhu T, Liang J, et al. Cu doping and Ti_3C_2OH quantum dots co-modifications of $Zn_3In_2S_6$ boosted photocatalytic reduction of CO_2 to CO via accelerating carriers transfer and enhancing CO_2 adsorption and activation. *Chem Eng J*. 2023;**452**: 139522.

45 Xie K, Umezawa N, Zhang N, Reunchan P, Zhang Y, Ye J. Self-doped $SrTiO_{3-\delta}$ photocatalyst with enhanced activity for artificial photosynthesis under visible light. *Energy Environ Sci*. 2011;**4**(10):4211–4219.

46 Kamat PV, Jin S. Semiconductor photocatalysis: "tell us the complete story!". *ACS Energy Lett*. 2018;**3**(3):622–623.

47 Tang H, Wang X, Yao C, Zhang Z. 0D/3D heterostructure of perovskite Cs_2CuBr_4 quantum dots/Bi_2O_3 microflower as a step-scheme photocatalyst for enhanced CO_2 reduction. *Sep Purif Technol*. 2024;**338**: 126544.

48 Shipman MA, Symes MD. Recent progress towards the electrosynthesis of ammonia from sustainable resources. *Catal Today*. 2017;**286**: 57–68.

49 Bu TA, Hao YC, Gao WY, Su X, Chen LW, Zhang N, et al. Promoting photocatalytic nitrogen fixation with alkali metal cations and plasmonic nanocrystals. *Nanoscale*. 2019;**11**(20):10072–10079.

50 Andrade PH, Volkringer C, Loiseau T, Tejeda A, Hureau M, Moissette A. Band gap analysis in MOF materials: distinguishing direct and indirect transitions using UV–vis spectroscopy. *Appl Mater Today*. 2024;**37**: 102094.

51 Gangu KK, Maddila S, Jonnalagadda SB. A review on novel composites of MWCNTs mediated semiconducting materials as photocatalysts in water treatment. *Sci Total Environ*. 2019;**646**: 1398–1412.

52 Luo J, Zhang S, Sun M, Yang L, Luo S, Crittenden JC. A critical review on energy conversion and environmental remediation of photocatalysts with remodeling crystal lattice, surface, and interface. *ACS Nano*. 2019;**13**(9):9811–9840.

53 Shahzad MK, Farooq MU, Laghari RA, Khan MA, Tahir MB, Azeem W, et al. Investigation of structural, electronic, mechanical, & optical characteristics of Ra based-cubic hydrides $RbRaX_3$ (X = F and cl) perovskite materials for solar cell applications: first principle study. *Heliyon*. 2023;**9**(7):e18407.

54 Miodyńska M, Kaczmarczyk O, Lisowski W, Żak A, Klimczuk T, Paszkiewicz M, et al. Encapsulation of $Cs_3Bi_2Br_9$ perovskite photocatalyst with polythiophene for prolonged activity in oxidizing and humid environment. *Appl Surf Sci*. 2024;**643**: 158725.

55 Nawaz A, Ali S, Atif M, Naz F, Khan A, Nian L, et al. A robust rationally designed multinarydouble perovskites microplates as an efficient visible-light photocatalyst. *Surf Interfaces*. 2023;**38**: 102794.

56 Li C, Xu X, Liu M, He S, Qian Y, Li Z. Oxygen-vacancy-rich porous perovskite as a photocatalyst: reducing reactive oxygen species quenching to improve peroxysulfate utilization. *J Water Process Eng*. 2024;**60**: 105142.

57 Pattanayak P, Singh P, Bansal NK, Paul M, Dixit H, Porwal S, et al. Recent progress in perovskite transition metal oxide-based photocatalyst and photoelectrode materials for solar-driven water splitting. *J Environ Chem Eng*. 2022;**10**(5):108429.

58 Bae S, Kim S, Lee S, Choi W. Dye decolorization test for the activity assessment of visible light photocatalysts: realities and limitations. *Catal Today*. 2014;**224**: 21–28.

59 Zhou Y, Lu F, Fang T, Gu D, Feng X, Song T, et al. A brief review on metal halide perovskite photocatalysts: history, applications and prospects. *J Alloys Compd*. 2022;**911**: 165062.

60 Shvalyuk DN, Shelyapina MG, Zvereva IA. Electronic structure and water induced phase transformation in layered perovskite-like $K_2La_2Ti_3O_{10}$ photocatalyst for water splitting studied by DFT. *J Phys Chem Solids*. 2023;**179**: 111384.

61 Nagaveni K, Sivalingam G, Hegde MS, Madras G. Solar photocatalytic degradation of dyes: high activity of combustion synthesized nano TiO_2. *Appl Catal B: Environ*. 2004;**48**(2):83–93.

62 Siddiquey IA, Furusawa T, Sato M, Honda K, Suzuki N. Control of the photocatalytic activity of TiO_2 nanoparticles by silica coating with polydiethoxysiloxane. *Dyes Pigm*. 2008;**76**(3):754–759.

63 Pozzo RL, Baltanas MA, Cassano AE. Supported titanium oxide as photocatalyst in water decontamination: state of the art. *Catal Today*. 1997;**39**(3):219–231.

64 Shi JB, Wu PF, Lin HS, Lin YT, Lee HW, Kao CT, et al. Synthesis and characterization of single-crystalline zinc tin oxide nanowires. *Nanoscale Res Lett*. 2014;**9**: 1–6.

65 Pozzo RL, Giombi JL, Baltanás MA, Cassano AE. The performance in a fluidized bed reactor of photocatalysts immobilized onto inert supports. *Catal Today*. 2000;**62**(2–3):175–187.

66 Zhang H, Quan X, Chen S, Zhao H, Zhao Y. Fabrication of photocatalytic membrane and evaluation its efficiency in removal of organic pollutants from water. *Sep Purif Technol*. 2006;**50**(2):147–155.

67 Lee DK, Kim SC, Cho IC, Kim SJ, Kim SW. Photocatalytic oxidation of microcystin-LR in a fluidized bed reactor having TiO_2-coated activated carbon. *Sep Purif Technol*. 2004;**34**(1–3):59–66.

68 Chong MN, Vimonses V, Lei S, Jin B, Chow C, Saint C. Synthesis and characterisation of novel titania impregnated kaolinite nano-photocatalyst. *Microporous Mesoporous Mater*. 2009;**117**(1–2):233–242.

69 Zhang H, Quan X, Chen S, Zhao H, Zhao Y. Fabrication of photocatalytic membrane and evaluation its efficiency in removal of organic pollutants from water. *Sep Purif Technol*. 2006;**50**(2):147–155.

70 Zhang X, Du AJ, Lee P, Sun DD, Leckie JO. Grafted multifunctional titanium dioxide nanotube membrane: separation and photodegradation of aquatic pollutant. *Appl Catal B: Environ*. 2008;**84**(1–2):262–267.

71 Vinodgopal K, Wynkoop DE, Kamat PV. Environmental photochemistry on semiconductor surfaces: photosensitized degradation of a textile azo dye, acid orange 7, on TiO_2 particles using visible light. *Environ Sci Technol*. 1996;**30**(5):1660–1666.

72 Fujishima A, Zhang X, Tryk DA. TiO_2 photocatalysis and related surface phenomena. *Surf Sci Rep*. 2008;**63**(12):515–582.

73 Wang J, Ku X, Lin J. Numerical investigation of biomass pyrolysis performance in a fluidized-bed reactor by a TFM-DEM hybrid model. *Chem Eng Sci*. 2022;**260**: 117922.

74 Pareek V, Chong S, Tadé M, Adesina AA. Light intensity distribution in heterogenous photocatalytic reactors. *Asia-Pacific J Chem Eng*. 2008;**3**(2):171–201.

75 de Oliveira AE, Visioli LJ, Enzweiler H. Photocatalytic reactors and their scale up: literature review. *CIS-Conjecturas Inter Studies*. 2022;**22**(6):509–530.

76 Molinari R, Grande C, Drioli E, Palmisano L, Schiavello M. Photocatalytic membrane reactors for degradation of organic pollutants in water. *Catal Today*. 2001;**67**(1–3):273–279.

77 Chin SS, Chiang K, Fane AG. The stability of polymeric membranes in a TiO_2 photocatalysis process. *J Membr Sci*. 2006;**275**(1–2):202–211.

78 Molinari R, Palmisano L, Drioli E, Schiavello M. Studies on various reactor configurations for coupling photocatalysis and membrane processes in water purification. *J Membr Sci*. 2002;**206**(1–2):399–415.

79 Gernjak W, Fuerhacker M, Fernández-Ibañez P, Blanco J, Malato S. Solar photo-Fenton treatment—process parameters and process control. *Appl Catal B: Environ*. 2006;**64**(1–2):121–130.

80 Andreozzi R, Caprio V, Insola A, Marotta R. Advanced oxidation processes (AOP) for water purification and recovery. *Catal Today*. 1999;**53**(1):51–59.

81 Consoli F, Allen D, Boustead I, Fava J, Franklin W, Jensen AA, et al. Guidelines for life-cycle assessment: a “Code of practice”. In: *SETAC Workshop*. vol. 31, Sesimbra, Portugal: Society of Environmental Toxicology and Chemistry (SETAC); 1993, March.

82 Muñoz I, Peral J, Ayllón JA, Malato S, Passarinho P, Domènech X. Life cycle assessment of a coupled solar photocatalytic–biological process for wastewater treatment. *Water Res*. 2006;**40**(19):3533–3540.

83 Munawar T, Mukhtar F, Batoo KM, Mazhar A, Nadeem MS, Hussain S, et al. Sunlight-activated Mo-doped La_2CuO_4/rGO perovskite oxide nanocomposite for photocatalytic treatment of diverse dyes pollutant. *Mater Sci Eng: B*. 2024;**304**: 117355.

84 Keshipour S, Hadidi M, Gholipour O. A review on hydrogen generation by photo-, electro-, and photoelectro-catalysts based on chitosan, chitin, cellulose, and carbon materials obtained from these biopolymers. *Adv Polym Technol*. 2023;**2023**(1):8835940.

85 Tailor NK, Singh S, Afroz MA, Pant KK, Satapathi S. Unraveling the impact of Cu-doping in lead free halide perovskites for markedly enhancing photocatalytic CO_2 reduction performance. *Appl Catal B: Environ*. 2024;**340**: 123247.

86 Liu X, Jing X, Liu R, Guo P, Yin Z. Plasmon-enhanced perovskite photocatalysts for CO_2 reduction: a mini review. *Energy Fuels*. 2024;**38**(6):4966–4979.

87 Kobayakawa K, Teranishi A, Tsurumaki T, Sato Y, Fujishima A. Photocatalytic activity of $CuInS_2$ and $CuIn_5S_8$. *Electrochim Acta*. 1992;**37**(3):465–467.

88 Schrader ML, Schäfer FR, Schäfers F, Glorius F. Bridging the information gap in organic chemical reactions. *Nat Chem*. 2024;**16**(4):491–498.

89 Lewis NS. Light work with water. *Nature*. 2001;**414**(6864):589–590.

90 Jafari T, Moharreri E, Amin AS, Miao R, Song W and Suib SL. Photocatalytic water splitting—The untamed dream: A review of recent advances. *Molecules*. 2016;**21**(7):900. Available from: https://doi.org/10.3390/molecules21070900

91 Ikeda S, Itani T, Nango K, Matsumura M. Overall water splitting on tungsten-based photocatalysts with defect pyrochlore structure. *Catal Lett*. 2004;**98**: 229–233.

92 Miodyńska M, Kaczmarczyk O, Lisowski W, Żak A, Klimczuk T, Paszkiewicz M, et al. Encapsulation of $Cs_3Bi_2Br_9$ perovskite photocatalyst with polythiophene for prolonged activity in oxidizing and humid environment. *Appl Surf Sci*. 2024;**643**: 158725.

93 Liton MNH, Roknuzzaman M, Helal MA, Kamruzzaman M, Islam AKMFU, Ostrikov K, et al. Electronic, mechanical, optical and photocatalytic properties of perovskite $RbSr_2Nb_3O_{10}$ compound. *J Alloys Compd*. 2021;**867**: 159077.

94 Boulahouache A, Benlembarek M, Salhi N, Djaballah AM, Rabia C, Trari M. Preparation, characterization and electronic properties of $LaFeO_3$ perovskite as photocatalyst for hydrogen production. *Int J Hydrogen Energy*. 2023;**48**(39):14650–14658.

95 Zhou T, Zhai T, Shen H, Wang J, Min R, Ma K, et al. Strategies for enhancing performance of perovskite bismuth ferrite photocatalysts ($BiFeO_3$): a comprehensive review. *Chemosphere*. 2023;**339**: 139678.

96 Kuspanov Z, Umirzakov A, Serik A, Baimenov A, Yeleuov M, Daulbayev C. Multifunctional strontium titanate perovskite-based composite photocatalysts for energy conversion and other applications. *Int J Hydrogen Energy*. 2023;**48**(98):38634–38654.

97 Ling CM, Mohamed AR, Bhatia S. Performance of photocatalytic reactors using immobilized TiO_2 film for the degradation of phenol and methylene blue dye present in water stream. *Chemosphere*. 2004;**57**(7):547–554.

98 Gelover S, Gómez LA, Reyes K, Leal MT. A practical demonstration of water disinfection using TiO_2 films and sunlight. *Water Res*. 2006;**40**(17):3274–3280.

99 Crittenden JC, Zhang Y, Hand DW, Perram DL, Marchand EG. Solar detoxification of fuel-contaminated groundwater using fixed-bed photocatalysts. *Water Environ Res*. 1996;**68**(3):270–278.

100 Rinco'n AG, Pulgarin C. Effect of pH, inorganic ions, organic matter and H_2O_2 on *E. coli* K_{12} photocatalytic inactivation by TiO_2-implications in solar water disinfection. *Appl Catal B: Environ*. 2004;**51**: 283–302.

101 Herrmann JM. Heterogeneous photocatalysis: fundamentals and applications to the removal of various types of aqueous pollutants. *Catal Today*. 1999;**53**: 115–129.

102 Kerzhentsev M, Guillard C, Herrmann JM, Pichat P. Photocatalytic pollutant removal in water at room temperature: case study of the total degradation of the insecticide fenitrothion (phosphorothioic acid O, O-dimethyl-O-(3-methyl-4-nitro-phenyl) ester). *Catal Today*. 1996;**27**: 215–220.

103 Habibi MH, Hassanzadeh A, Mahdavi S. The effect of operational parameters on the photocatalytic degradation of three textile azo dyes in aqueous TiO_2 suspensions. *J Photochem Photobiol A: Chem*. 2005;**172**: 89–96.

104 Martin ST, Lee AT, Hoffmann MR. Chemical mechanism of inorganic oxidants in the TiO_2/UV process: increased rates of degradation of chlorinated hydrocarbons. *Environ Sci Technol*. 1995;**29**: 2567–2573.

105 Shahzad MK, Mujtaba ST, Hussain S, Rehman JU, Farooq MU, Khan MA, et al. Zirconium-based cubic-perovskite materials for photocatalytic solar cell applications: a DFT study. *RSC Adv*. 2022;**12**(42):27517–27524.

106 Zhou Z, Li Q, Su G, Pang J, Sun B, Meng J, et al. Catalytic degradation of chlorinated volatile organic compounds (CVOCs) over Ce–Mn–Ti composite oxide catalysts. *J Environ Sci*. 2024;**138**: 326–338.

107 Shahzad MK, Hussain S, Farooq MU, Laghari RA, Bilal MH, Khan SA, et al. First-principles calculations to investigate structural, electronic, elastic and optical properties of radium based cubic fluoro-perovskite materials. *Heliyon*. 2023;**9**(2):e13687.

108 Shahzad MK, Mujtaba ST, Hussain S, Farooq MU, Laghari RA, Khan SA, et al. Lithium-based perovskites materials for photovoltaic solar cell and protective rays window applications: a first-principle calculations. *Discov Nano*. 2023;**18**(1):15.

109 Shaheen SE, Brabec CJ, Sariciftci NS, Padinger F, Fromherz T, Hummelen JC. 2.5% efficient organic plastic solar cells. *Appl Phys Lett*. 2001;**78**(6):841–843.

110 Hauch JA, Schilinsky P, Choulis SA, Childers R, Biele M, Brabec CJ. Flexible organic P3HT: PCBM bulk-heterojunction modules with more than 1 year outdoor lifetime. *Sol Energy Mater Solar Cells*. 2008;**92**(7):727–731.

111 Yu G, Gao J, Hummelen JC, Wudl F, Heeger AJ. Polymer photovoltaic cells: enhanced efficiencies via a network of internal donor-acceptor heterojunctions. *Science*. 1995;**270**(5243):1789–1791.

112 Peumans P, Uchida S, Forrest SR. Efficient bulk heterojunction photovoltaic cells using small-molecular-weight organic thin films. *Nature*. 2003;**425**(6954):158–162.

113 Gan Q, Bartoli FJ, Kafafi ZH. Plasmonic-enhanced organic photovoltaics: breaking the 10% efficiency barrier. *Adv Mater*. 2013;**25**(17):2385–2396.

114 Dou L, You J, Hong Z, Xu Z, Li G, Street RA, et al. 25th anniversary article: a decade of organic/polymeric photovoltaic research. *Adv Mater*. 2013;**25**(46):6642–6671.

115 Clarke TM, Durrant JR. Charge photogeneration in organic solar cells. *Chem Rev*. 2010;**110**(11):6736–6767.

116 Tang CW. Two-layer organic photovoltaic cell. *Appl Phys Lett*. 1986;**48**(2):183–185.

117 Wang Y, Feng M, Chen H, Ren M, Wang H, Miao Y, et al. Highly crystalized Cl-Doped SnO_2 nanocrystals for stable aqueous dispersion toward high-performance perovskite photovoltaics. *Adv Mater*. 2024;**36**(5):2305849.

118 Huang J, Xiang H, Ran R, Zhou W, Wang W, Shao Z. Fundamental understanding in the performance-limiting factors of $Cs_2AgBiBr_6$-based perovskite photovoltaics. *Renew Sustain Energy Rev*. 2024;**191**: 114187.

119 Ciesielski PN, Hijazi FM, Scott AM, Faulkner CJ, Beard L, Emmett K, et al. Photosystem I–based biohybrid photoelectrochemical cells. *Bioresour Technol*. 2010;**101**(9):3047–3053.

120 Eperon GE, Stranks SD, Menelaou C, Johnston MB, Herz LM, Snaith HJ. Formamidinium lead trihalide: a broadly tunable perovskite for efficient planar heterojunction solar cells. *Energy Environ Sci*. 2014;**7**(3):982–988.

121 Chen Q, Zhou H, Hong Z, Luo S, Duan HS, Wang HH, et al. Planar heterojunction perovskite solar cells via vapor-assisted solution process. *J Am Chem Soc*. 2014;**136**(2):622–625.

122 Conibeer G. Third-generation photovoltaics. *Mater Today*. 2007;**10**(11):42–50.

123 Araújo GL, Martí A. Absolute limiting efficiencies for photovoltaic energy conversion. *Sol Energy Mater Sol Cells*. 1994;**33**(2):213–240.

124 Song Z, Abate A, Watthage SC, Liyanage GK, Phillips AB, Steiner U, et al. Perovskite solar cell stability in humid air: partially reversible phase transitions in the $PbI_2–CH_3NH_3I–H_2O$ system. *Adv Energy Mater*. 2016;**6**(19):1600846.

125 Roose B, Baena JPC, Gödel KC, Graetzel M, Hagfeldt A, Steiner U, et al. Mesoporous SnO_2 electron selective contact enables UV-stable perovskite solar cells. *Nano Energy*. 2016;**30**: 517–522.

126 Hadadian M, Correa-Baena JP, Goharshadi EK, Ummadisingu A, Seo JY, Luo J, et al. Enhancing efficiency of perovskite solar cells via N-doped graphene: crystal modification and surface passivation. *Adv Mater*. 2016;**28**(39):8681–8686.

127 Geens W, Aernouts T, Poortmans J, Hadziioannou G. Organic co-evaporated films of a PPV-pentamer and C_{60}: model systems for donor/acceptor polymer blends. *Thin Solid Films*. 2002;**403**: 438–443.

128 Shaheen SE, Radspinner R, Peyghambarian N, Jabbour GE. Fabrication of bulk heterojunction plastic solar cells by screen printing. *Appl Phys Lett*. 2001;**79**(18):2996–2998.

129 Li B, Li S, Gong J, Wu X, Li Z, Gao D, et al. Fundamental understanding of stability for halide perovskite photovoltaics: the importance of interfaces. *Chem*. 2024;**10**(1):35–47.

130 Lin M, Xu X, Tian H, Yang Y, Sha WE, Zhong W. Quantifying nonradiative recombination and resistive losses in perovskite photovoltaics: a modified diode model approach. *Solar RRL*. 2024;**8**(1):2300722.

131 Sun Z, Popa D, Hasan T, Torrisi F, Wang F, Kelleher EJ, et al. A stable, wideband tunable, near transform-limited, graphene-mode-locked, ultrafast laser. *Nano Res*. 2010;**3**: 653–660.

132 Franklin AD, Luisier M, Han SJ, Tulevski G, Breslin CM, Gignac L, et al. Sub-10 nm carbon nanotube transistor. *Nano Lett*. 2012;**12**(2):758–762.

133 Ando T, Nakanishi T. Impurity scattering in carbon nanotubes–absence of back scattering. *J Phys Soc Jpn*. 1998;**67**(5):1704–1713.

134 Peluso P, Sechi B, Jibuti G. Enantioseparation of organometallic compounds by electromigration techniques. *Electrophoresis*. 2024;**45**(11–12):1018–1032.

135 Datta S. *Electronic transport in mesoscopic systems*. Cambridge: Cambridge University Press; 1997.

136 Chen Z, Appenzeller J, Knoch J, Lin YM, Avouris P. The role of metal-nanotube contact in the performance of carbon nanotube field-effect transistors. *Nano Lett*. 2005;**5**(7):1497–1502.

137 Wang F, Dukovic G, Brus LE, Heinz TF. Time-resolved fluorescence of carbon nanotubes and its implication for radiative lifetimes. *Phys Rev Lett*. 2004;**92**(17):177401.

138 Misewich JA, Martel R, Avouris P, Tsang JC, Heinze S, Tersoff J. Electrically induced optical emission from a carbon nanotube FET. *Science*. 2003;**300**(5620):783–786.

139 Gao S, Liu W, Wang M, Zhao Z, Liu X. A three-dimensional in-situ self-electrolysis system based on $Ni_3(HITP)_2$/graphene-based composite aerogel particle electrodes for efficient deep removal of phenol from coking wastewater. *Appl Catal B: Environ*. 2024;**340**: 123276.

140 Huang Q, Tian S, Zeng D, Wang X, Song W, Li Y, et al. Enhanced photocatalytic activity of chemically bonded TiO_2/graphene composites based on the effective interfacial charge transfer through the C–Ti bond. *ACS Catal*. 2013;**3**(7):1477–1485.

141 Attia AK. Photolysis and photocatalysis of methylene blue by graphene oxide nanoparticle under sunlight irradiation. *J College Basic Educ*. 2024;**30**(123):46–56.

142 Cao A, Liu Z, Chu S, Wu M, Ye Z, Cai Z, et al. A facile one-step method to produce graphene–CdS quantum dot nanocomposites as promising optoelectronic materials. *Adv Mater*. 2010;**22**(1):103–106.

143 Pastrana-Martínez LM, Morales-Torres S, Likodimos V, Figueiredo JL, Faria JL, Falaras P, et al. Advanced nanostructured photocatalysts based on reduced graphene oxide–TiO_2 composites for degradation of diphenhydramine pharmaceutical and methyl orange dye. *Appl Catal B: Environ*. 2012;**123**: 241–256.

144 Liu X, Cong R, Cao L, Liu S, Cui H. The structure, morphology and photocatalytic activity of graphene–TiO_2 multilayer films and charge transfer at the interface. *New J Chem*. 2014;**38**(6):2362–2367.

145 World Health Organization. Prevention and control of dengue and dengue haemorrhagic fever (No. Regional Publication No. 29). WHO Regional Office for South-East Asia; 1999.

146 Pereira GV, Freitas VA, Oliveira HS, Oliveira LCA, Belchior JC. A photocatalytic process for the eradication of dengue through' OH generation in the presence of sunlight and iron oxide. *RSC Adv*. 2014;**4**(109):63650–63654.

147 Tang Z, Butkus MA, Xie YF. Enhanced performance of crumb rubber filtration for ballast water treatment. *Chemosphere*. 2009;**74**(10):1396–1399.

148 Dunlop PSM, Byrne JA, Manga N, Eggins BR. The photocatalytic removal of bacterial pollutants from drinking water. *J Photochem Photobiol A: Chem*. 2002;**148**(1–3):355–363.

149 Ono I, Oku T, Suzuki A, Fukunishi S, Tachikawa T, Hasegawa T. Effects of ethylammonium and rubidium addition to guanidinium-based $CH_3NH_3PbI_3$ perovskite photovoltaic devices prepared at 190 °C in ambient air. *Mater Today Commun*. 2024;**38**: 107623.

150 Jin RJ, Lou YH, Huang L, Wang KL, Chen CH, Chen J, et al. Photochemical shield enabling highly efficient perovskite photovoltaics. *Adv Mater*. 2024;**36**(21):2313154.

151 Somoza-Tornos A, Guerra OJ, Crow AM, Smith WA, Hodge BM. Process modeling, techno-economic assessment, and life cycle assessment of the electrochemical reduction of CO_2: a review. *Iscience*. 2021;**24**(7):102813.

152 Shi G, Huang Z, Qiao R, Chen W, Li Z, Li Y, et al. Manipulating solvent fluidic dynamics for large-area perovskite film-formation and white light-emitting diodes. *Nat Commun*. 2024;**15**(1):1066.

153 Li B, Li S, Gong J, Wu X, Li Z, Gao D, et al. Fundamental understanding of stability for halide perovskite photovoltaics: the importance of interfaces. *Chem*. 2024;**10**(1):35–47.

154 Shen L, Wu H, Cao Z, Zhang X, Liu L, Sawwan H, et al. Two-dimensional metal halide perovskites created by binary conjugated organic cations for high-performance perovskite photovoltaics. *ACS Appl Mater Interfaces*. 2024;**16**(15):19318–19329.

155 Li J, Ji S, Wei H, Gong J, Mao W, Zhang W, et al. Multifunctional one-dimensional seeding layers enable stable and over 20%-efficiency inverted perovskite photovoltaic modules. *Nano Energy*. 2024;**122**: 109329.

156 Jiménez-López MA, Rey A, Rivas FJ, Beltrán FJ. Water ozone decomposition in graphitic and graphene based catalytic materials: kinetics of catalyst deactivation. *Catal Today*. 2024;**430**: 114541.

157 Assad H, Lone IA, Kumar A, Kumar A. Unveiling the contemporary progress of graphene-based nanomaterials with a particular focus on the removal of contaminants from water: a comprehensive review. *Front Chem*. 2024;**12**: 1347129.

158 Saini R, Naaz F, Bashal AH, Pandit AH, Farooq U. Recent advances in nitrogen-doped graphene-based heterostructures and composites: mechanism and active sites for electrochemical ORR and HER. *Green Chem*. 2024;**26**: 57–102.

159 Ali I, Hasan SZ, Garcia H, Danquah MK, Imanova G. Recent advances in graphene-based nano-membranes for desalination. *Chem Eng J*. 2024;**483**: 149108.

160 Mehew JD, Unal S, Torres Alonso E, Jones GF, Fadhil Ramadhan S, Craciun MF, et al. Fast and highly sensitive ionic-polymer-gated WS2–graphene photodetectors. *Adv Mater*. 2017;**29**(23):1700222.

161 Chen W, Kaya Özdemir Ş, Zhao G, Wiersig J, Yang L. Exceptional points enhance sensing in an optical microcavity. *Nature*. 2017;**548**(7666):192–196.

162 Öz S, Singh T, Resalati S, Kim GM, Babu V. Industrial perspectives on the upscaling of perovskite materials for photovoltaic applications and its environmental impacts. In: *Metal halide perovskites for generation, manipulation and detection of light*. Amsterdam: Elsevier; 2023. p. 117–142.

163 Li J, Wu N. Semiconductor-based photocatalysts and photoelectrochemical cells for solar fuel generation: a review. *Catal Sci Technol*. 2015;**5**(3):1360–1384.